Copyright Warning & Restrictions

The copyright law of the United States (Title 17, United States Code) governs the making of photocopies or other reproductions of copyrighted material.

Under certain conditions specified in the law, libraries and archives are authorized to furnish a photocopy or other reproduction. One of these specified conditions is that the photocopy or reproduction is not to be "used for any purpose other than private study, scholarship, or research." If a, user makes a request for, or later uses, a photocopy or reproduction for purposes in excess of "fair use" that user may be liable for copyright infringement,

This institution reserves the right to refuse to accept a copying order if, in its judgment, fulfillment of the order would involve violation of copyright law.

Please Note: The author retains the copyright while the New Jersey Institute of Technology reserves the right to distribute this thesis or dissertation

Printing note: If you do not wish to print this page, then select "Pages from: first page # to: last page #" on the print dialog screen

ABSTRACT

HEART RATE VARIABILITY STUDIES ON AMBULATORY SUBJECTS USING EKG DERIVED RESPIRATION

by
Xiaorui Tang

Power spectral analysis of heart rate variability (HRV) provides a powerful non-invasive tool for exploring the balance between sympathetic and parasympathetic components of the autonomic nervous system. In the spectrum of HRV, there are three distinct peaks. The high frequency (HF) band (0.15 to 0.4 Hz) is correlated with parasympathetic activity and this is the band of interest in the study.

Two groups of subjects were considered in this work, stroke survivors and subjects performing an oral presentation in front of an audience. Data were collected with a Holter monitor to allow for ambulatory recording. Respiration was derived from the EKG and was used to determine the parasympathetic frequency band in the HRV spectrum.

The power spectral analysis of HRV from stroke survivors revealed significantly less parasympathetic activity than in control subjects. Sustained low variation of heart rate suggested that stroke survivors may suffer from one or more aspects of autonomic nervous system imbalance.

The power spectral analysis of HRV from normal subjects during a formal presentation revealed that vagal activity decreased significantly with the anticipation of making a presentation as well as during the presentation in the presence of an audience, when compared to vagal activity during a presentation without an audience.

HEART RATE VARIABILITY STUDIES ON AMBULATORY SUBJECTS USING EKG DERIVED RESPIRATION

by
Xiaorui Tang

A Thesis
Submitted to the Faculty of
New Jersey Institute of Technology
in Partial Fulfillment of the Requirements for the Degree of
Master of Science in Electrical Engineering

Department of Electrical and Computer Engineering

January 1995

APPROVAL PAGE

HEART RATE VARIABILITY STUDIES ON AMBULATORY SUBJECTS USING EKG DERIVED RESPIRATION

Xiaorui Tang

Dr. Stanley S. Reisman, Thesis Advisor — Date
Professor of Electrical and Computer Engineering
Associate Chairperson for Graduate Studies, NJIT

Dr. Peter Engler, Committee Member — Date
Associate Professor of Electrical and Computer
Engineering, NJIT

Dr. Thomas W. Findley, Committee Member — Date
Associate Professor of Physical
Medicine and Rehabilitation, UMDNJ
Director of Research, Kessler Institute for
Rehabilitation

BIOGRAPHICAL SKETCH

Author: Xiaorui Tang

Degree Master of Science in Electrical Engineering

Date January 1995

Undergraduate and Graduate Education:

- Master of Science in Electrical Engineering
  New Jersey Institute of Technology, Newark, NJ, 1995

- Bachelor of Science in Information and Electronic Science
  Yunnan University, Yunnan, P. R. China, 1989

Major: Electrical Engineering

This thesis is dedicated to my beloved parents
Ruiming Xia and Guiyao Tang
and also
all the people who have ever helped and encouraged me

ACKNOWLEDGMENT

I am grateful for the help and the support provided by Dr. Stanley S. Reisman, without whom this thesis never would have been completed.

Special thanks to Dr. Thomas W. Findley and Dr. Peter Engler for serving as members of the committee.

TABLE OF CONTENTS

Chapter	Page
1 INTRODUCTION	1
1.1 Heart, Electrocardiogram and Heart Rate Variability	1
1.2 Power Spectral Analysis of Heart Rate Variability	7
1.3 Derivation of Respiration from EKG during Heart Rate Variability Studies	12
1.4 Power Spectral Analysis of 24-Hour Heart Rate Variability	15
1.5 Scope of the Thesis	16
2 METHODS	18
2.1 Data Acquisition	18
2.2 Subjects and Experimental Procedures	21
2.2.1 Subjects and Experimental Set-up for Stroke Survivor Test	21
2.2.2 Subjects and Experimental Procedures for Presentation Test	23
2.3 Data Analysis	24
3 RESULTS	26
3.1 Results of Stroke Survivor Test	26
3.1.1 Vagal Activities	26
3.1.2 Box Plot of HRV	31
3.2 Results of Oral Presentation Test	39
3.3 Cross Correlation of EKG-derived Respiration With Directly Measured Respiration	43

TABLE OF CONTENTS
(Continued)

Chapter **Page**

3.3.1 Understanding of the Cross Correlation 44

3.3.2 Cross Correlation of EKG Derived Respiration with Original Respiration 52

3.4 Fidelity of Holter recorder Playback System 56

3.5 Variables May Affect the Quality of Holter Data Processing 59

3.5.1 Speed Variation of Holter System 59

3.5.2 Presence of Premature Beats in the Holter R-R Interval Data 60

4 DISCUSSION AND CONCLUSIONS 71

4.1 Low Vagal Activities in Stroke Survivors 71

4.2 Less Heart Rate Variations in Stroke Survivors 72

4.3 Vagal Activities Change with the Respiration Rate 73

4.4 Vagal Withdraw with Audience 74

5 FUTURE WORKS 76

APPENDIX A PROCEDURE FOR CALCULATING VAGAL ACTIVITY 79

APPENDIX B PROCEDURE FOR DERIVING RESPIRATION FROM EKG 81

APPENDIX C S-PLUS PROGRAMS 82

REFERENCES 94

LIST OF TABLES

Table **Page**

2.1 Conversion between recording time and playing back time.....20

3.1 Differences in HRV power between stroke survivors and control subjects.....30

3.2 High frequency area values.....41

3.3 Low frequency area values.....42

3.4 Very low frequency area values.....42

3.5 LF:HF ratio values.....43

LIST OF FIGURES

Figure **Page**

1.1 The atria and the ventricles of the heart, showing also the sinus node, the AV node,and the ventricular bundle branches....1

1.2 Configuration of a typical electrocardiogram, illustrating the important deflections and intervals....2

1.3 Standard bipolar leads for recording EKG....3

1.4 Diagram depicting the nerve supple to the heart from both divisions of the Autonomic Nervous System....4

1.5 Power spectrum of heart rate fluctuations, indicating low-frequency, mid-frequency, and high-frequency peaks....9

1.6 Different lead EKG signals influenced by respiration.... 12

1.7 Axis of the mean QRS vector influenced by respiration.... 14

2.1 QRS complex area....25

3.1 Power spectrum of HRV and power spectrum of EKG-derived respiration.... 27

3.2 Box plots of the IBIs of one pair of subjects for overall test stages....32

3.3 Box plots of IBIs of 6 pairs of subjects for 8bpm paced breathing test.... 36

3.4 Areas to be calculated....40

3.5 Graphic illustration of correlation.... 45

3.6 Cross correlation of two same sine waves....49

3.7 Cross correlation of two different sine waves.... 50

3.8 Cross correlation of two sine waves, one wave is contained in the other.... 50

3.9 Cross correlation of two sine waves which are 180° out of the phase....51

LIST OF FIGURES
(Continued)

Figure **Page**

3.10 Cross correlation of two sine waves which contain DC component..... 51

3.11 Cross correlation of the EKG derived respiration with the original respiration.....53

3.12 Cross correlation of the spectrum of the EKG derived respiration with the spectrum of the original respiration.....54

3.13 Respiration signals which cause low cross correlation..... 55

3.14 Comparison of different play back systems..... 58

3.15 Comparison of original and Holter recorded EKG signals and their spectra..... 58

3.16 Premature contraction.....61

3.17 The affect of premature contraction on the HR spectrum..... 62

3.18 Cubic interpolation..... 63

CHAPTER 1

INTRODUCTION

1.1 Heart, Electrocardiogram and Heart Rate Variability

The heart, illustrated in Figure 1.1, consists of two separate pumps: a right side that pumps the blood through the lungs and a left side that pumps the blood through all tissues in the body except the lungs[1][2]. In turn, each of these two separate sides of the heart is a pulsatile two-chamber pump composed of an atrium and a ventricle.

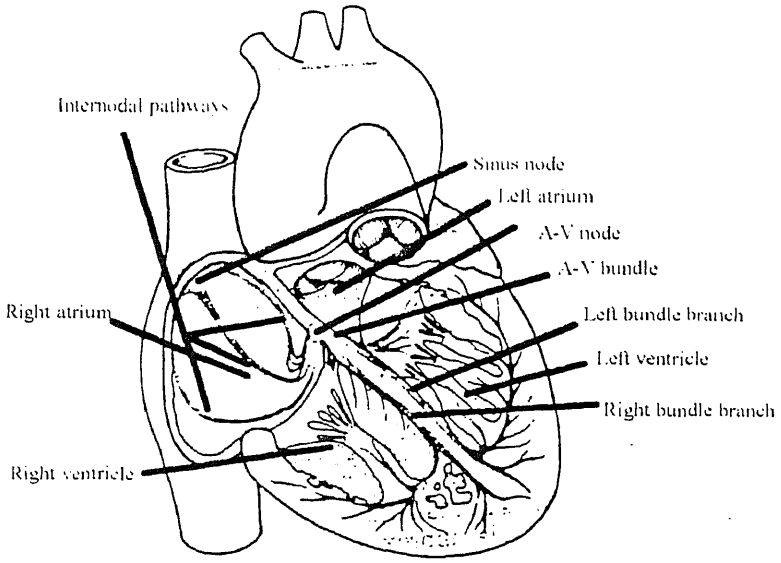

Figure 1.1 The atria and the ventricles of the heart, showing also the sinus node, the AV node, and the ventricular bundle branches

Special mechanisms in the heart maintain cardiac rhythmicity and transmit action potentials throughout the heart muscle to cause periodic heart beats. Each period is initiated by spontaneous generation of an action potential in the sinoatrial (SA) node, which is located in the superior lateral wall of the right atrium near the opening of the superior vena cava. Because the cells of the SA node are autorhythmic, the SA node is designated as a pacemaker. From the SA node, the action potential travels rapidly to the atrioventricular (AV) node, which is situated near the top of the ventricular septum and activates the bundle of His which divides into two branches serving the right and left ventricles. Through these branches the action potential finally passes to the ventricles and generates ventricular contraction.

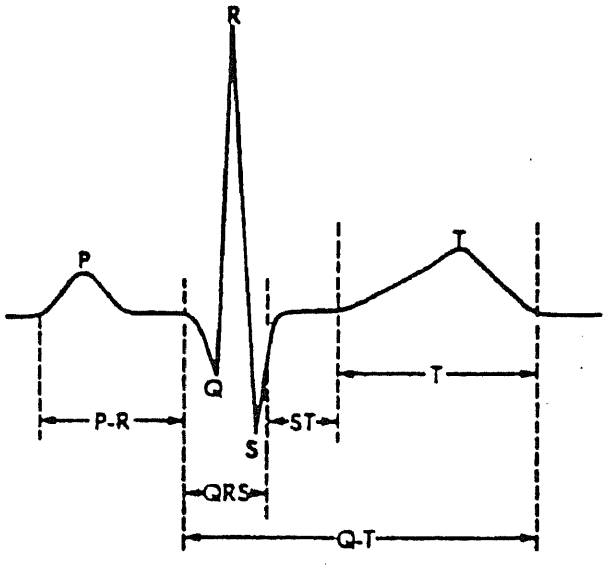

Figure 1.2 Configuration of a typical electrocardiogram, illustrating the important deflections and intervals.

The electrocardiogram (ECG or EKG) is primarily a tool for evaluating the electrical events within the heart. The sum of the action potentials occurring simultaneously in many individual cells can be detected by recording electrodes at the surface of the skin. Figure 1.2 illustrates a typical normal EKG signal. It consists of P, QRS, and T waves. They represent atrial contraction, ventricular contraction and ventricular relaxation respectively

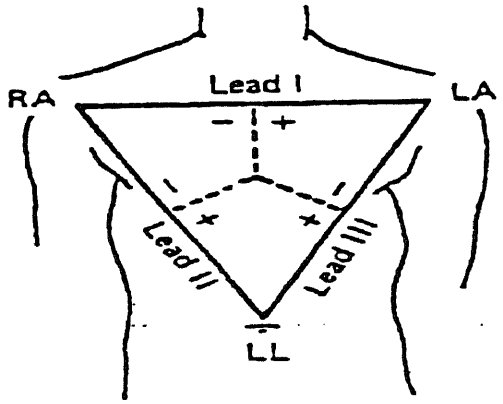

Figure 1.3 Standard bipolar leads for recording EKG

In Figure 1.3, the standard bipolar limb leads for recording the EKG is illustrated. The term "bipolar" means that the EKG is recorded from two specific electrodes on the body. Thus, a "lead" is not a single wire attached to the body but a combination of two wires and their electrodes to make a complete circuit with the EKG monitor. In recording lead I, the negative terminal of the EKG monitor is connected to the right arm and the positive terminal to the left arm. In recording lead II, the negative terminal is connected to the right arm and the positive

terminal to the left leg. In recording lead III, the negative terminal is connected to the left arm and the positive terminal to the left leg. The reference point (ground) is connected to the right leg. We are assuming that lead I (RA-LA) and lead III (LA-LL) form an orthogonal set which is necessary to derive the respiration from the EKG (See section 1.3)

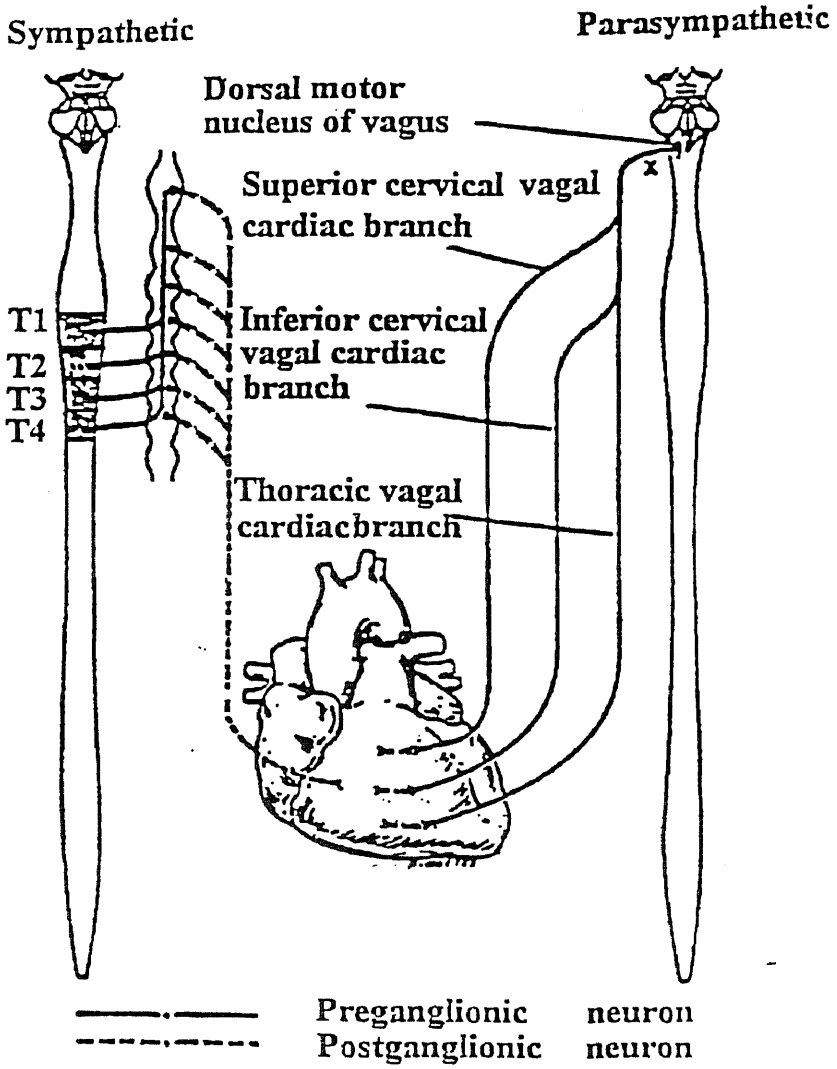

Figure 1.4 Diagram depicting the nerve supply to the heart from both divisions of the Autonomic Nervous System

For the normal individual, how fast the heart beats depends totally on how fast the SA node is depolarized. In other words, the depolarization rate of the SA node determines the heart rate. Usually, the SA node is under the influence of the autonomic nervous system.

The autonomic nervous system is a part of the nervous system which is concerned with control of involuntary body functions[3]. It helps control arterial pressure, heart rate, body temperature and many other activities. The autonomic nervous system is activated mainly by centers located in the spinal cord, brain stem, and hypothalamus. Also, portions of cerebral cortex, especially of the limbic cortex, can transmit impulses to the lower centers and in this way influence autonomic control. The efferent autonomic signals are transmitted to the body through two major subdivisions called the sympathetic nervous system and the parasympathetic nervous system. Figure 1.4 depicts the nerve supply to the heart from both branches of the nervous system. Sympathetic fibers terminate at the SA node, conduction system, atria, ventricles and coronary vessels, while, parasympathetic fibers terminate at the SA node, atrioventricular (AV) node, atria, ventricles and coronary vessels. The sympathetic nervous system increases the heart rate and the parasympathetic nervous system decreases the heart rate. One of the most striking characteristics of the autonomic nervous system is the rapidity and intensity with which it can change visceral functions. Strong sympathetic stimulation can increase the heart rate in the human to as high as 200 and rarely even 250 beats per minute in young people. Strong parasympathetic stimulation of

the heart can actually stop the heartbeat for a few seconds, but then the heart usually "escapes" and beats at a rate of 20 to 30 beats per minute thereafter.

Changes in heart rate reflect the reciprocal action of the sympathetic and parasympathetic systems. The spontaneous fluctuations in heart rate are normally considered a healthy sign. Wide variations in heart rate are commonly seen in healthy individuals. By contrast, a number of physiologic and disease states produce alterations in autonomic function which reduce the variability in heart rate[4]. In one HRV study, Pagani et al. subjected 49 uncomplicated diabetics and 40 age-matched controls to supine and tilt conditions while recording their HRV[5]. The R-R variance was reduced during both rest and tilt in diabetics. This observation suggested poor parasympathetic activation in diabetic patients. In another landmark study, Kleiger et al. observed that in a large sample (N=808) of post myocardial infarction (MI) patients, a low (<50 msec)standard deviation of mean R-R interval over 24h duration, 2 weeks after the MI, had the strongest univariate correlation with mortality[6]. The relative risk of mortality was 5.3 times higher in the group with low HRV (<50 msec) than the group with high HRV (>100 msec). It is hypothesized that decreased HRV correlates with increased sympathetic tone and decreased vagal tone and thus predisposes the patient to ventricular fibrillation[7]. Other recent studies also showed that the heart rate of patients with severe coronary artery disease, congestive heart failure, aging, and hypertension often varies less than that of normal people[8]. Therefore, to some extent, wide variation of heart rate could be considered as one of the healthy indicators. HRV analysis could also make a positive contribution to identify

sympathvagal imbalance. Implicit in these studies is the assumption that HRV study may shed light on the physiological mechanisms underlying the disorder.

1.2 . Power Spectral Analysis of Heart Rate Variability

Power spectral analysis of heart rate variability (HRV) is a potentially powerful tool for exploring neurocardiac dysfunction, in patients with a variety of cardiac and autonomic disorders. The power spectral analysis process transforms a signal from the time domain to the frequency domain. It provides a window through which neurocardiac and autonomic function can be assessed noninvasively[9].

According to signal processing theory, Fourier series can be used to represent all periodic functions, that is, all periodic functions can be represented as a sum of sins and cosines at a fundamental frequency and its harmonics.

The Fourier series of a function f(t) is represented as[26]:

$$f(t) = \frac{a_0}{2} + \sum_{n=1}^{\infty} \left(a_n \cos\frac{n\pi}{l} t + b_n \sin\frac{n\pi}{l} t\right) \tag{1.1}$$

where

$$a_n = \frac{1}{l}\int_{-l}^{l} f(t)\cos\frac{n\pi}{l} t\,dt \qquad (n=0,1,2...) \tag{1.2}$$

$$b_n = \frac{1}{l}\int_{-l}^{l} f(t)\sin\frac{n\pi}{l} t\,dt \qquad (n=0,1,2...) \tag{1.3}$$

When functions are not periodic, Fourier series are expanded to the Fourier transform to accommodate non-periodic functions. Using Fourier transform techniques, the frequency components of a non-periodic function, which may be

present at all frequencies, can be represented.

If $\int_{-\infty}^{\infty}|f(t)|dt$ converges, and f(t) is piecewise continuous on $[-\infty,\infty]$, the Fourier transform of f(t) is defined as:

$$F(\omega)=\int_{-\infty}^{\infty}f(t)e^{-j\omega t}dt \tag{1.4}$$

In the above definition, we assume that f(t) is a piecewise continuous function. This implies that:

1. $\lim_{t\to-\infty+} f(t)$ and $\lim_{t\to+\infty-} f(t)$ are finite.

2. f(x) is continuous at all but possible finite number of points on $[-\infty,\infty]$.

3. At any point in $[-\infty,\infty]$ where f(t) is discontinuous, the function has finite left and right limits.

A non-mathematical analogy of the Fourier transform is that of a glass prism which splits white light up into a rainbow. This represents the different spectral , or frequency components that make up the white light, and the prism is acting to separate the white light into its characteristic frequencies.

The following steps are used to perform power spectral analysis of HRV[12]. First, every R wave position in the ECG signal is detected by setting appropriate threshold values, and an interbeat interval signal (IBI) is generated by taking the difference in time between successive R waves and converting the measured time to an IBI amplitude. Since an IBI only occurs when the R wave is

measured time to an IBI amplitude. Since an IBI only occurs when the R wave is detected, the width of the IBI samples is not constant. In order to produce IBI samples of equal width suitable for analysis, a backward step function interpolation method is used to interpolate the IBI samples. Then, the frequency components of the IBI signal are estimated by taking the Fourier transform of the interpolated IBI signal. The detail is discussed in section 2.2.

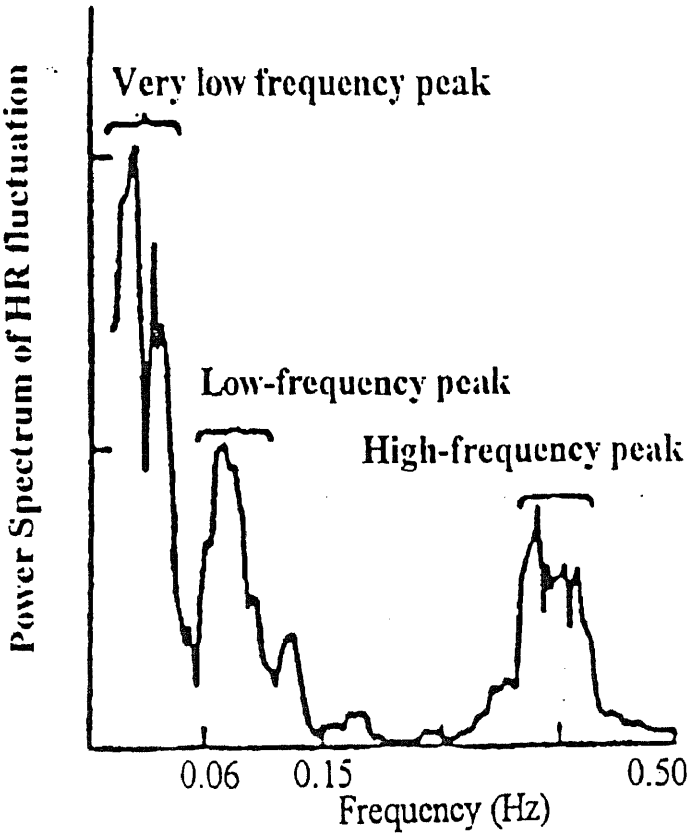

Figure 1.5 Power spectrum of heart rate fluctuations, indicating low-frequency, mid-frequency, and high-frequency peaks.

Figure 1.5 illustrates the conversion of a sequence of consecutive R-R intervals into its spectral components in a normal subject. Three peaks are visible: a very low frequency peak (0.0033 Hz-0.04 Hz), a low frequency peak (0.04 Hz-0.15 Hz) and a high frequency peak (0.15 Hz- 0.4 Hz). These three peaks have generally been assumed to represent different systems influencing heart rate. The very low-frequency band is correlated with vasomotor control and/or temperature control. The low frequency band is associated with baroreceptor-mediated blood pressure control and the high-frequency band has been linked with respiration[4].

At this time, in power spectral analysis of heart rate variability, the best-known and best-defined peak is the peak at the respiration frequency, which is called the respiration peak. A century ago, the influence of respiratory variation on heart rate, so-called respiratory sinus arrhythmia (RSA), was recognized well by Ludwing[11]. RSA is a rhythmical fluctuation in heart periods at the respiratory frequency that is characterized by a shortening and lengthening of heart periods in a phase relationship with inspiration and expiration. Over the past decade, an increasing number of psychological, physiological and clinical studies have utilized RSA as an index of vagal control of the heart. The potential utility of RSA as a non invasive index of vagal influence on the heart assumes special importance in view of the emerging understanding of the complexities of autonomic control. In the power spectral analysis of heart rate variability, the respiration peak corresponds approximately to the RSA, and it is purely parasympathetic in origin[12]. Individual differences of area values under respiration peaks have been interpreted as differences in basal cardiac vagal tone, and within-subject changes

of area values under respiration peaks have been suggested to correspond to alterations in this vagal tone. This interpretation is based partially on the fact that changes in vagal activity may yield corresponding changes in area values under respiration peaks. Important considerations arise in the finding of the respiration peak. The normal respiration rates vary considerably from individual to individual. The normal respiration rate can be as low as only a few breaths per minute at rest and as high as up to 40 breathes per minute during intense exercise[1]. Thus, the frequencies of spontaneous respiration are not limited to the narrow band ranging from 0.15 Hz to 0.4 Hz, and may cover a wider range. If the respiration peak has moved out of the narrow band (0.15 Hz-0.4 Hz), and we calculate the power within the frequency band of 0.15 Hz to 0.4 Hz as the measure of vagal tone activity, the results would be completely wrong. Therefore, in order to correctly measure vagal activity, the original respiration signal has to be available. However, in some cases, we do not have respiration information. For example, when we use Holter Monitor (which is a small three-channel cassette recorder designed to record an ambulatory subject's EKG continuously for up to 24 hours.) to collect EKG data, respiration information is not available. In this situation, power spectral analysis of heart rate variability is greatly limited.

In order to avoid the above limitation of power spectral analysis of HRV, Zhao, Reisman, and Findley recently (1994) proposed a new approach, which is called ECG derived respiration, to be used when the respiration signal is not available. By using the EKG derived respiration technique, we can generate a respiration signal from the raw EKG data.

1.3 Derivation of Respiration from ECG during Heart Rate Variability Studies

ECG derived respiration is an indirect method to reconstruct respiration information from ECG signals. A biological signal is often influenced by many interacting systems. For instance, an EKG signal, besides being created by the cardiac system, is also influenced by the respiratory system. This feature makes it possible to derive a specific biological signal from a signal generated by one of its interacting systems, and the EKG derived respiration algorithm is based on this feature. The EKG derived respiration algorithm is based on the observation that the ECG is influenced by electrode motion relative to the heart and that fluctuations in the mean cardiac electrical axis accompany respiration[8].

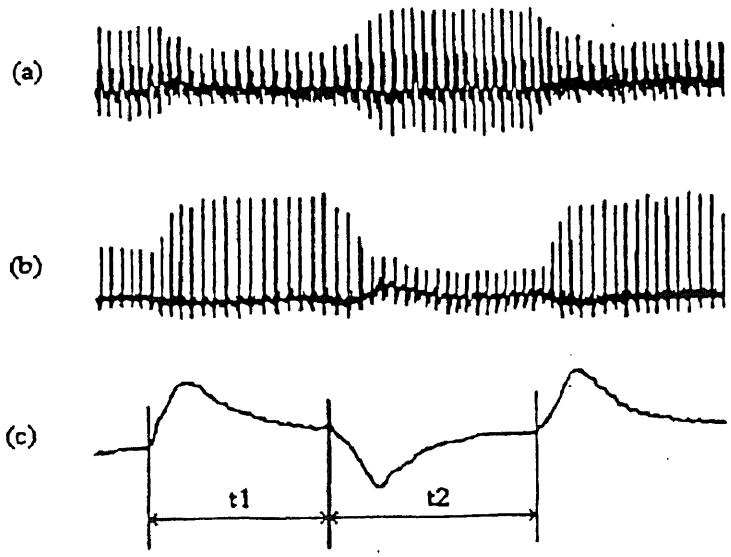

Figure 1.6 Different lead EKG signals influenced by respiration. (a): lead I EKG; (b): lead III EKG; (c): respiration; t1: deep inhalation and hold; t2: deep exhalation and hold

In the ECG derived respiration method, ECG signals from lead I and from lead III are used. Figure 1.6 illustrates the influences of respiration on lead I and lead III EKGs.

In time period t1, the subject was asked to perform a deep inhalation and hold . During this period, the amplitude of lead I is decreased and that of lead III is increased. In time period t2, the subject was asked to perform a deep exhalation and hold . During this period, the amplitude of lead I is increased and that of lead III is decreased significantly. The reason that the amplitudes of lead I and lead III always move in the opposite direction can be explained by the anatomical changes of the heart in the chest during respiration. During inhalation and hold, because of the filling of the lungs, the apex of the heart is turned towards the abdomen. As a result, the cardiac vector in the longitudinal direction represented by lead III is increased, and the cardiac vector in the crosswise direction represented by lead I is decreased. Conversely, during exhalation and hold, because of the emptying of the lungs, the apex of the heart is turned towards the chest. This makes the cardiac vector in longitudinal direction (lead III) decreased and the cardiac vector in crosswise direction (lead I) increased. Figure 1.6 demonstrates the amplitude of cardiac vectors change in lead I and lead III.

In the ECG derived respiration technique, the area of each normal QRS complex in each of the two leads is measured over a fixed time window. Since the window width is fixed, the area is proportional to the amplitude of the ECG signal.

The QRS area generated from a certain lead can be also considered as a QRS vector, which has the same direction as that lead direction. The arc tangent of the ratio of the areas measured in leads I and III yields the angle of the mean axis of QRS vector with respect to one of the lead axes. The projection of the mean QRS vector is proportional to the projection of the mean cardiac electrical vector on the lead axis. The angle values are interpolated to produce a continuous ECG-derived respiratory signal.

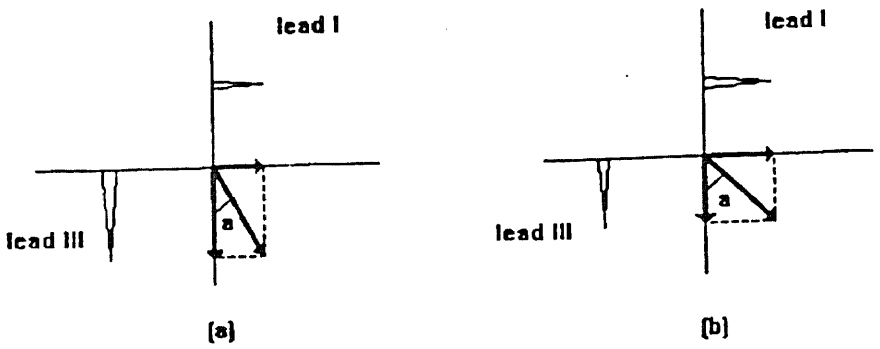

Figure 1.7 Axis of the mean QRS vector influenced by respiration. a: the angle of the axis respect to the lead III axis. (a): deep inhalation and hold; (b): deep exhalation and hold

Zhao and Reisman proved a strong association between the major peak of the original respiration spectrum and that of the derived respiration spectrum. The detail of their work is discussed in section 4.1.

1.4. Power Spectral Analysis of 24-Hour Heart Rate Variability

In order to obtain the neurocardiac control information in health and disease, during normal life, throughout the day, more and more ECG data are taken from ambulatory subjects. Twenty-four-hour recordings of ECG have become an established monitoring and diagnostic tool in clinical cardiology.

In 1992, Bigger, et al. performed power spectral analyses on the entire twenty-four-hour ECG data from 715 myocardial infarction patients in order to test the hypothesis that short-term power spectral measures of heart rate variability will predict cardiac mortality or arrhythmic death [14]. Four frequency domain measures were calculated from spectral analyses of heart period over a twenty-four-hour interval. They computed the twenty-four-hour power spectral density and calculated the power within three frequency bands: (1) 0.0033 to < 0.04 Hz, very low frequency power, (2) 0.04 to < 0.15 Hz, low frequency power, and (3) 0.15 to 0.4 Hz, high frequency power. In addition, they calculated the ratio of low to high frequency power. These measures were calculated for 15, 10, 5 and 2 minute segments during the day and at night. Their study shows that mean power spectral values from short periods during the day and night were similar to twenty-four-hour values, and the correlation between short segment values and twenty-four hour values were strong (many correlations were ≥ 0.75). Therefore, power spectral measures of HRV calculated from short (2 to 15 minutes) EKG recordings are remarkably similar to those calculated over 24 hours. The power spectral measures of HRV are excellent predictors of all-cause mortality and sudden cardiac death.

In 1994, Fei, et al, performed spectral analyses on twenty-four-hour EKG data from 10 patients with aborted sudden cardiac attack not associated with coronary artery disease, in order to make an assessment of heart rate variability in survivors of sudden cardiac attack not associated with coronary artery disease[15]. Spectral heart rate variability was analyzed on a Holter analysis system and was expressed as total (0.01 - 1.00 Hz), low (0.04 - 0.15 Hz) and high (0.15 - 0.4 Hz) frequency components for each hour. HRV was calculated for the 24 hour periods. Their findings suggest that there is abnormal autonomic influence on the heart in patients without coronary artery disease at risk of sudden cardiac attack. Hourly analyses of HRV throughout the 24 hour period may provide additional information important in the identification of high risk patients.

1.5 Scope of the Thesis

In this study, we used short term (2 minutes) power spectral analysis to assess HRV in stroke survivors and HRV in people doing oral presentation under varying conditions.

In the stroke survivor experiment, we tested the hypothesis that stroke survivors have lower parasympathetic activity than normal controls. The data from this experiment were treated as the pilot data for a project set up by a physician at Kesseler Institute for Rehabilitation. The purpose of the project is to determine whether parasympathetic function, as measured by heart rate variability, can predict adverse cardiac events in stroke survivors during the first year post stroke.

It has been shown that certain cardiac conditions can lead directly to stroke, and stroke also may lead to cardiac disorders[16]. Heart disease and stroke both are associated with common risk factors, including hypertension, hyperlipidemia, cigarette smoking, diabetes, obesity, sedentary lift style, type A personality, older age, and male gender. Due to deconditioning during the acute recovery period and difficulty with exercise using paralyzed or spastic extremities, stroke survivors may experience heart rate increase up to 73% of age-predicated maximum during exercise, and are likely to experience abnormalities in heart rate [17]. Cardiac abnormalities have been found in at least 50% of stroke survivors. Due to the above mentioned factors, it becomes very important to predict adverse cardiac events in stroke survivors.

In order to find the association between HRV and adverse cardiac events in stroke survivors, HRV needs to be measured 4, 26, and 52 weeks after the stroke. Although the data in this study are only a small portion of the data that needed to be collected for the original project, results of this study have already shown that stroke survivors have lower parasympathetic activity than normal controls.

In the oral presentation experiment, we tested the hypotheses that the presence of an audience will affect autonomic behavior. It has been shown that the complex social facts, such as mere presence or observation, can affect behavior and health[18], but little is known about how these social facts affect the human physiology. The data from this experiment will illustrate for the first time the social-psychological influence on the autonomic nervous system.

CHAPTER 2

METHODS

2.1 Data Acquisition

In both stroke survivors and oral presentation tests, EKG signals were recorded using Model 459 Holter recorder (Cardio Corder, Model 459, Del Mar Avionics, Irvine, California). The Model 459 Holter is a small three-channel cassette designed to record an ambulatory subject's EKG continuously for up to 24 hours. It includes a patient's event button, an automatic calibrator, the patient electrode cables, the patient cable connector and a carrying case. A 9-volt disposable battery supplies power.

In our study, EKG signals were obtained from bipolar lead I and lead III attached to the subject. The leads consisted of two exploring electrodes, two reference electrodes and one ground electrode. When the Holter recorder power is turned on, six minutes of 1 mv calibration pulses are automatically recorded on two channels. During this six minute period, the Holter can not record any input signal. The internal calibration signal can be terminated by pressing the patient event button on the Holter. Once the calibration signal stops, the Holter recorder starts to record input signals. In order to distinguish each event when data was recovered from the Holter tape, the patient event button was pressed at the beginning of each different event during recording. During playback, the

oscilloscope was used to monitor the resulting EKG signals, and each event marker appeared as a sequence of square waves on the oscilloscope.

The Holter tape EKG signals were played back using a JVC TD-W10 consumer quality music cassette tape recorder with frequency response range from 30 Hz to 16000 Hz. The analog output of the JVC TD-W10 cassette was converted into a digital signal by a DAS-16 analog-to-digital converter (Keithley MetraByte/Asyst, Natick MA). The DAS-16 analog-to-digital converter is a full length board installed internally in an expansion slot of an IBM PC/XT/AT and compatibles to turn the computer into a fast, high-precision data acquisition and signal analysis instrument. The converted digital data were then stored on an IBM compatible 286 computer with 2Mb RAM and 170 Mb hard drive, using Streamer V3.25 data acquisition software (Keithley MetraByte/Asyst, Natick MA). 9.62 kHz sampling rate, which corresponds to 200 Hz sampling rate for the original EKGs, was used for acquiring data since the play back speed of the Holter is 48.1 times the recording speed.

The important issue in acquiring correct Holter data is to distinguish each event when the data is played back. Data on the Holter recorder was collected in two ways. In some situations, events were marked by the patient event marker and a time log was kept by the patient. However, in other protocols, a time log was kept only to mark experimental events on the Holter recorder. For the first case, since markers already exist on the tape, different events can be easily separated by counting the number of markers. For the second case where event markers do not exist, a time conversion must be made, where actual time is 1/48.1 of play back

time. In this case, in order to separate each event, a stop watch has to be prepared for counting play back time. Table 2.3.1 demonstrates an example of time conversion. In the table, The "Actual time" column indicates the start and the end record time of each phase, The "Time from the start" column indicates when a particular event begins with respect the total starting time. For example, the "time from the start" of sitting is 18m, which means that the sitting phase commenced 18 minutes after the total starting time. The "Conversion" column indicates the procedure of converting recording time to playing back time. The "Data acquiring time" column indicates the time at which data acquiring should be started. This time is related to the time at which stop watch is started.

Table 2.1 Conversion between recording time and playing back time

Actual Time	**Time from the start**	**Conversion**	**Data acquiring time**
Start 12:25	0(min)		0(s)
Sitting 12:43~12:48	18(min)	$\frac{18\times 60(s)}{48.1}=22.45(s)$	22.45(s)
Supine 1:18~1:23	58(min)	$\frac{53\times 60(s)}{48.1}=66.11(s)$	66.11(s)
Pace breathing 2:13~2:28	108(min)	$\frac{108\times 60(s)}{48.1}=134.7(s)$	134.7(s)

After being stored in the acquisition computer, the data was transferred to an IBM-compatible 485/66 MHz computer and was processed using the S-Plus for window V3.1 data analysis software package (Statistical Sciences, Seattle WA).

2.2. Subjects and Experimental Procedures

2.2.1 Subjects and Experimental Set-up for Stroke Survivor Test

The study of HRV in stroke survivors addresses the hypothesis that the parasympathetic (vagal) activity of stroke survivors is lower than that of normal subjects. This hypothesis is based on the consideration that most stroke survivors have cardiac risk, and people containing cardiac risk have low parasympathetic activity. Therefore, it is assumed that stroke survivors have low parasympathetic activity. In this study, we defined "normal" as a person without cardiac risk.

6 normal subjects and 6 stroke survivors took part in this study. These two groups were age and gender matched. Subjects covered a large age span, which is from 25 to 72 years old. Mean age of normal subjects was 47.8 years and was 50.83 years for stroke survivors. Subjects were excluded from the study if they were on sympatholytic or sympathomimetic medications. Each subject was tested in a quiet location in order to minimize external stressors. All tests were performed before lunch time.

Two lead EKG signals (lead I and lead III) were collected on subjects during 6 4-minutes test conditions: 1) sitting, non-paced breathing. 2) supine, non-paced breathing. 3) exercising. (subjects were instructed to exercise up to their normal comfortable level) 4) sitting, paced breathing at 8 **bpm**. 5) sitting, paced

breathing at 12 **bpm** and 6) sitting, paced breathing at 18 **bpm**. Before initiation of each phase, the patient button on the Holter recorder was pressed.

In this protocol, the sitting, non-paced breathing protocol corresponds to the time interval during which short-term measures of HRV are most easily obtained, because the subject is not asked to do anything unusual. The supine, non-paced breathing protocol represents a period of increased vagal tone. Exercising represents a period of very low, or no vagal tone. In the exercising test, both normal and stroke survivors were asked to exercise at their own comfortable normal level. If capable, subjects were instructed to exercise on a Kinetron Exercise and Training System (Cybex, Ronkonkema NY). Otherwise, subjects performed exercise by propelling a wheelchair.

Paced breathing is a method where subjects were forced to breath at a certain rate. The rate was controlled by a view box containing a column of lights that rose and fell at the desired breathing rate. The participant was instructed to match his/her breathing rate with the rate with which the light proceeded up and down the column. A light moving up directed subjects to breath in and a light moving down directed subjects to breath out. The paced breathing protocol was designed to accurately locate the parasympathetic peak in the power spectrum of HRV, and thus, to be able to estimate subject's parasympathetic activity accurately. As discussed in section 1.2, in the power spectrum of HRV, the high frequency band, from 0.15 Hz to 0.4 Hz, is associated with respiration, and is purely parasympathetic in origin. This occurs because the SA node's response to sympathetic activity is too slow to influence RSA when respiration is above 0.15

Hz[19]. However the natural respiration of individuals is unstable and irregular. The respiration frequency is not always in the 0.15 Hz to 0.4 Hz band. This makes it difficult to derive a relationship between natural respiration and heart rate and therefore makes it difficult to accurately identify the vagal peak in the power spectrum of HRV. The paced breathing protocol improve the situation by setting the breathing rate for every subject. In this way, the frequency band in which respiration occurs is determined, the position of the parasympathetic peak is determined, and therefore, the parasympathetic activity could be tested accurately.

2.2.2 Subjects and Experimental Procedure for Presentation Test

The presentation test was an experiment to determine how the presence and the size of audiences affect autonomic behavior. Six graduate students and one instructor participated in this investigation. None of the subjects were on sympatholytic or sympathomimetic medications. Each subject was asked to make one formal presentation of their current research in a research seminar class. During the 30 minute presentation the presenter was not interrupted. However, following the presentation pertinent questions and clarification were asked and suggestions were made by the audience. Later, the same presentations without audience were scheduled for all subjects. Each subject made the same presentation without the presence of the audience within one week. Data during anticipatory resting, presentation with audience and presentation without audience were recorded using the Holter recorder. Before initiation of each phase, the patient event button on the Holter recorder was pressed.

2.3 Data Analysis

In S-Plus, the power spectrum of the HRV was derived from the acquired EKG data by previously developed signal processing software algorithms[12]. In these algorithms, every QRS complex in the EKG signal is first detected, and the interbeat interval (IBI) was represented as the distance between two consecutive QRS complexes. Since IBI samples only occurred whenever an R wave was detected, they were not equidistant along the time axis. In order to produce equidistant IBI samples suitable for analysis, IBI samples were interpolated using a backward step interpolation function. In the backward step method, all of the interpolated values between a beat at time T(m-1) and the next beat at time T(m) are set equal to the time difference between T(m) and T(m-1). The heart rate variability signal used in this work is this interpolated IBI, which is called IIBI.

Sometimes very low frequency components caused either by the instruments used to acquire the signal or the subject's movements are contained in the IIBIs. Those very low frequency components smear the power spectrum of the signal at low frequencies. In order to remove the low frequency artifact, the IIBIs were detrended using a locally weighted robust regression algorithm. Finally, the power spectrum of HRV was formed by computing the FFT on the detrended IIBI.

In S-Plus, the respiration signal was derived by the algorithms developed by Zhao and Reisman[13]. In their algorithm, the area of each normal QRS complex in each of two leads was measured over a fixed time window. Figure 2.1 illustrates the area of the normal QRS complex and the window width fixed to compute the QRS complex area. Since the window was fixed, the area of each normal QRS was

proportional to the projection of the mean cardiac electrical vector on the lead axis. It was assumed that the lead I and the lead III used to derive respiration were orthogonal, so that the arc tangent of the ratio of the areas measured in the two leads yielded the angle of the mean axis of the QRS vector with respect to one of the lead axes. Since the angle samples only appeared whenever QRS complexes occurred, they were not equidistant along the time axis. In order to produce equidistant angle samples suitable for analysis, angle samples were interpolated by a cubic spline approximation. The interpolated angle samples were considered as a continuous EKG-derived respiratory signal. The spectrum of the derived respiration was produced by applying the FFT on the interpolated angle samples. Appendix A demonstrates all steps used to calculate the power spectrum of the HRV signal and Appendix B demonstrates all steps used to derive respiration from the EKG.

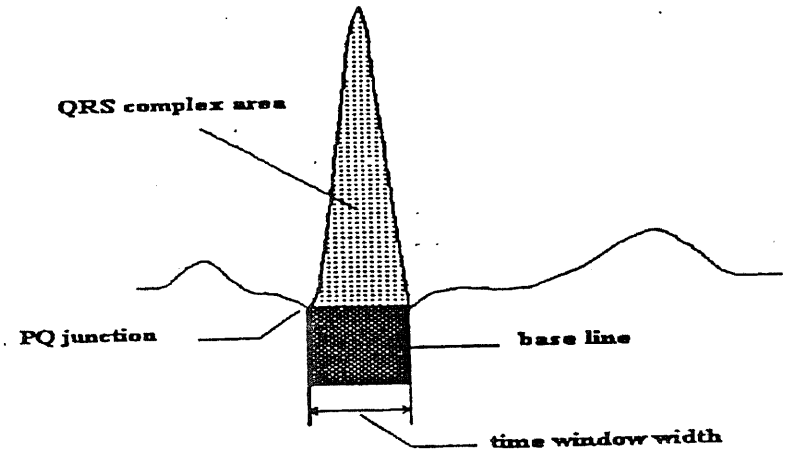

Figure 2.1 QRS complex area

CHAPTER 3

RESULTS

3.1 Result of Stroke Survivors Test

3.1.1 Vagal Activities

As previously discussed, in the power spectrum of HRV, there are three major peaks. The high frequency peak is correlated with respiration driven vagal efferent input to the sinus node. In this test, subject's parasympathetic (vagal) activities were measured by calculating the area under high frequency peak of the HRV spectrum. For all the tests, except 8bpm pacing and the exercise test, the high frequency peak was defined between 0.15 Hz and 0.4 Hz. However, considering that during 8bpm paced breathing, the subject's respiration frequency goes down to 0.13 Hz which is below 0.15 Hz, we defined the respiration related high frequency peak between 0.1 Hz and 0.4 Hz. Also, during the exercise test, since some subject's respiration frequencies could go higher than 0.4 Hz, we defined the high frequency peak between 0.15 Hz and 0.8 Hz.

Figure 3.1 shows the power spectrum of the HRV and the power spectrum of the EKG-derived respiration of one normal subject during each protocol stage. The X-axis reflects the frequency (Hz) and the Y- axis reflects the power density. The solid curve represents the power spectrum of the HRV, the dotted curve represents the power spectrum of the EKG-derived respiration, and the shaded parts represent the area where vagal activity values were estimated.

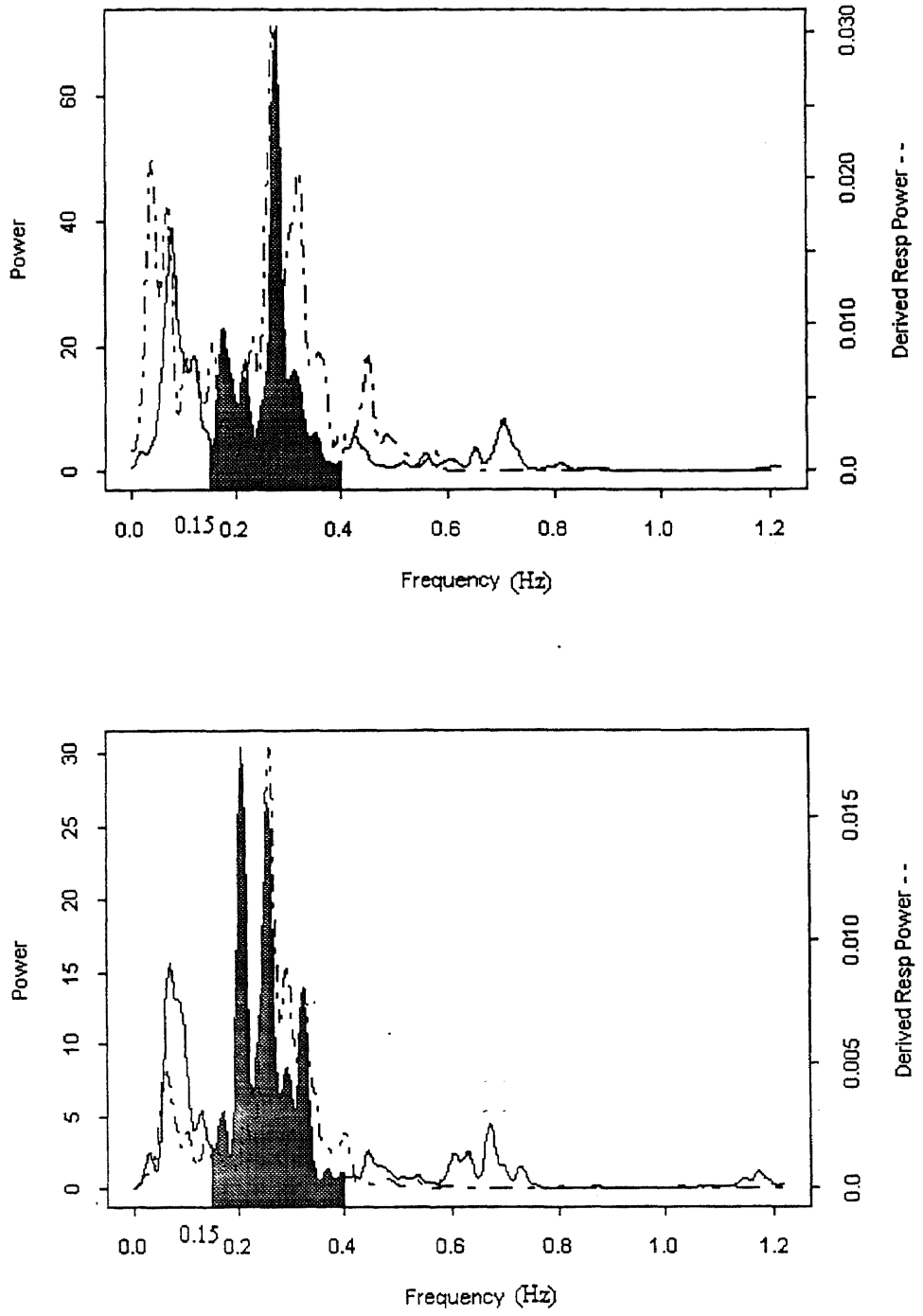

Figure 3.1 Power spectrum of HRV and power spectrum of EKG-derived respiration. a) Sitting, non-paced. b) Supine, non-paced.

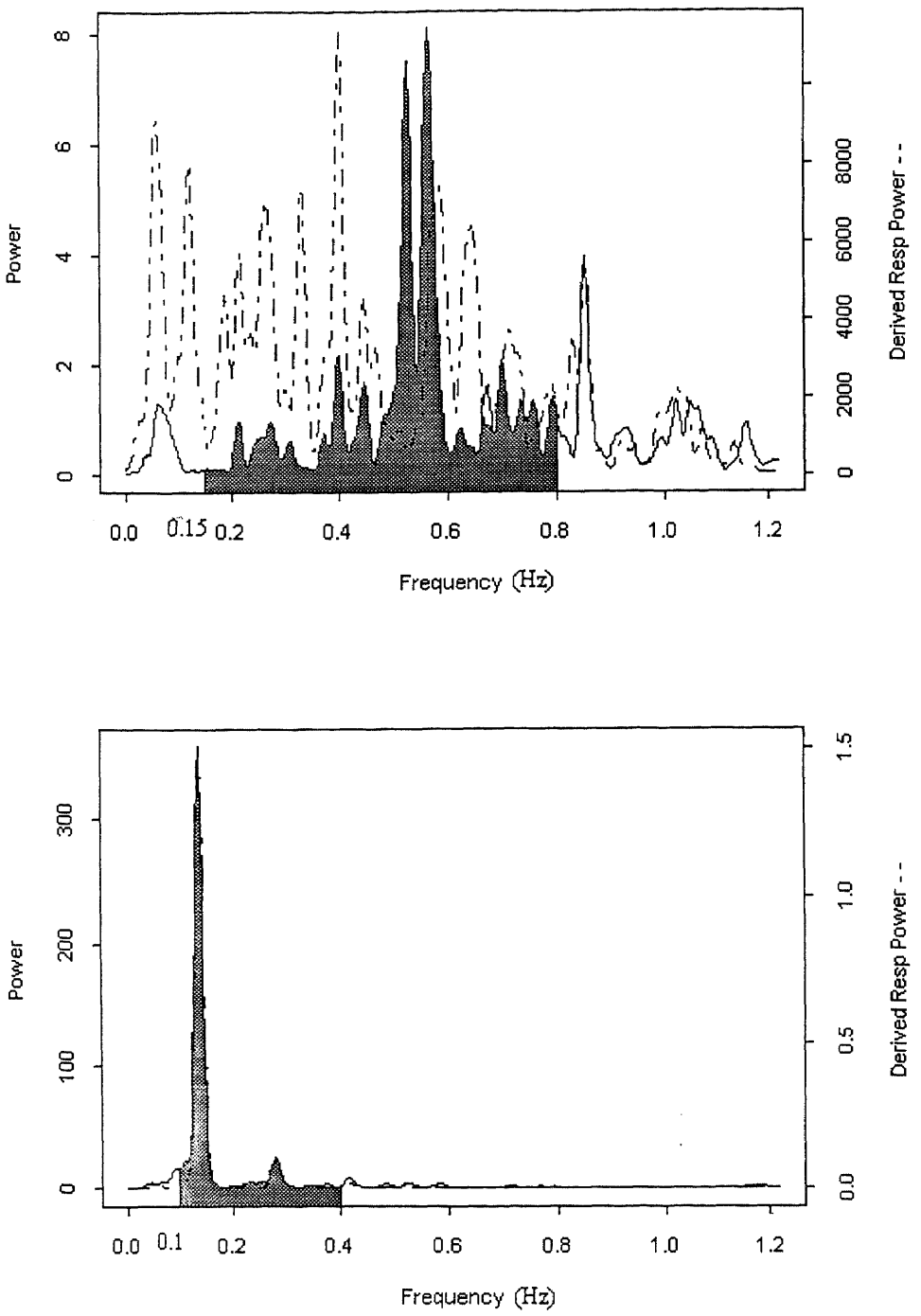

Figure 3.1 Power spectrum of HRV and power spectrum of EKG-derived respiration. c) Exercising. d) 8bpm

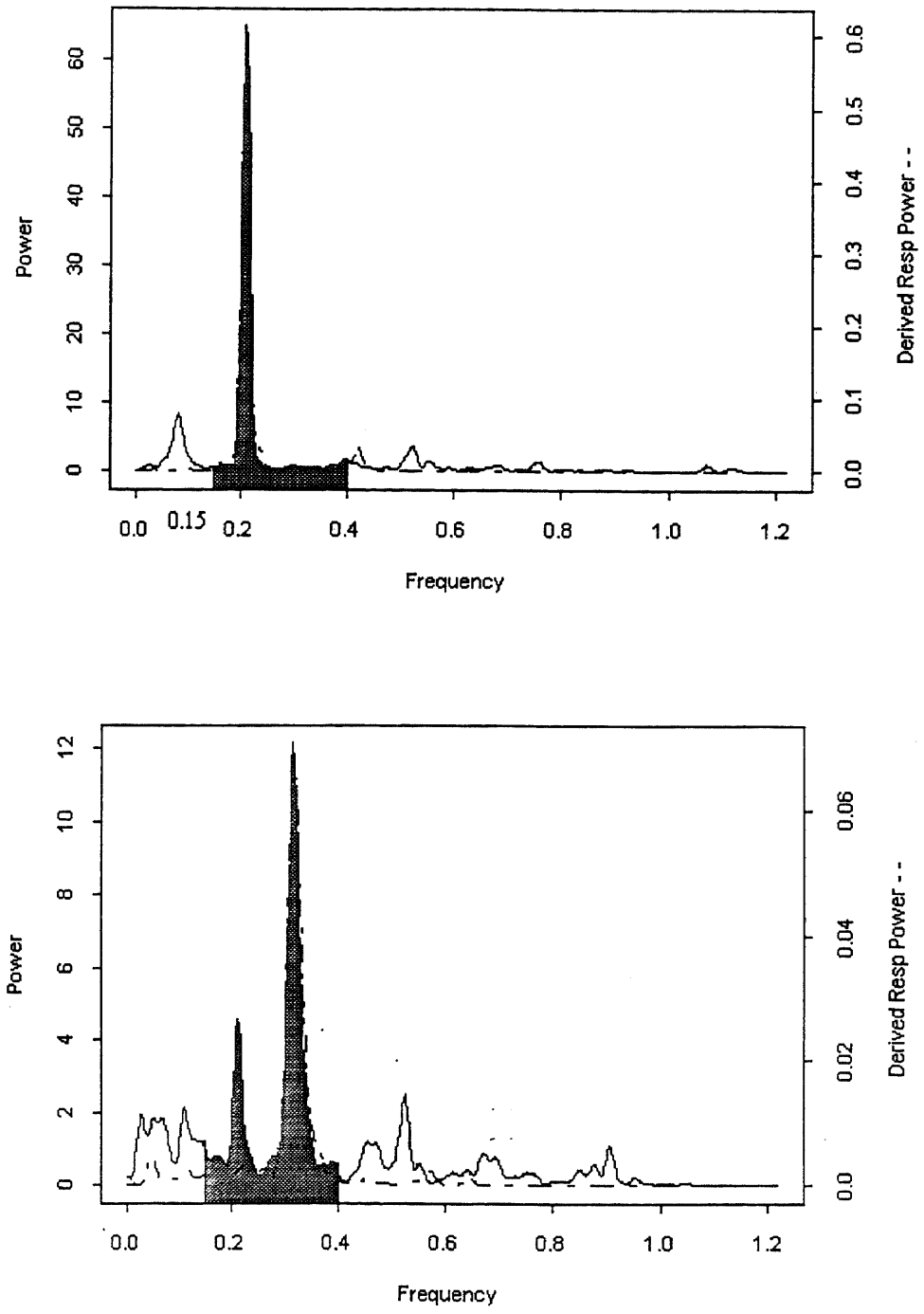

Figure 3.1 Power spectrum of HRV and power spectrum of EKG-derived respiration. e) 12bpm. f) 18 bpm

Table3.1 Differences in HRV power between stroke survivors and control subjects (pilot data)

AGE/SEX	HRV: Sitting	HRV: Supine	HRV: Exercise	PACED: 8 bpm	PACED: 12 bpm	PACED: 18 bpm
25/M	2.99	3.47	0.28	39.9	7.84	2.49
36/M	9.91	18.2	0.43	25.1	4.2	3.34
44/M	3.69	2.15	0.81	8.31	1.38	0.54
54/M	1.4	2.95	0.99	5.57	1.38	1.3
60/M	0.65	0.92	0.41	18.1	6.07	8.61
68/F	3.36	2.04	1.21	8.11	5.94	2.58
MEAN	3.67	4.96	0.69	17.52	4.47	3.14
S.D.	3.28	6.55	0.37	13.23	2.66	2.86

Table a. Normal Subjects.

AGE/SEX	HRV: Sitting	HRV: Supine	HRV: Exercise	PACED: 8 bpm	PACED: 12 bpm	PACED: 18 bpm
26/M	0.91	7.47	0.81	24.04	3.64	0.84
39/M	0.87	0.64	0.53	2.72	0.53	0.54
48/M	0.34	0.62	**	2.69	0.34	0.31
58/M	0.32	1.29	**	0.32	0.15	0.09
62/M	0.1	0.57	0.29	0.36	0.17	0.2
72/F	0.43	1.12	1.91	6.39	0.59	0.97
MEAN	0.50	1.95	0.59	6.09	0.90	0.49
S.D.	0.32	2.72	0.72	9.07	1.35	0.36

Table b. Stroke Survivors.

The vagal activity values for all subjects over all protocol stages are displayed in Table 3.1. During the exercise stage, the two vagal values marked with an asterisk were missing, because the EKG was poorly recorded by the Holter recorder due to sharp body movements during exercise. In both groups, mean and standard deviation values of all subjects are also displayed.

Multivariate analysis of variance (MANOVA) was performed by DeMeersman (unpublished) over all testing stages except EXERCISE due to 2 missing data points. Age was entered as a covariate. The overall effect was not significant ($p=0.217$), but the effect of stroke appeared to be approaching significant ($p=0.114$). The lack of significance may be due to the size of the sample. Post-hoc testing demonstrated significant group differences during NON-PACED: sitting ($p=0.049$) and PACED: 12bpm ($p=0.020$), but not during PACED: 8bpm ($p=0.071$), PACED: 18bpm ($p=0.053$) or NON-PACED: supine ($p=0.324$). A large sample size will be required to see significant differences between populations during individual interventions.

3.1.2 Box Plot of HRV

Box plots were used to demonstrate the difference of HRV between normal and stroke survivors. We separated our 12 subjects into 6 pairs, each pair containing an age and gender matched normal subject and a stroke survivor. Box plots of IBIs calculated from one pair of subjects over all test stages are shown in Figure 3.2. There are two boxes in each graph, where the boxes on the left side of each graph represent IBI data from normal subjects and the boxes on the right side represent

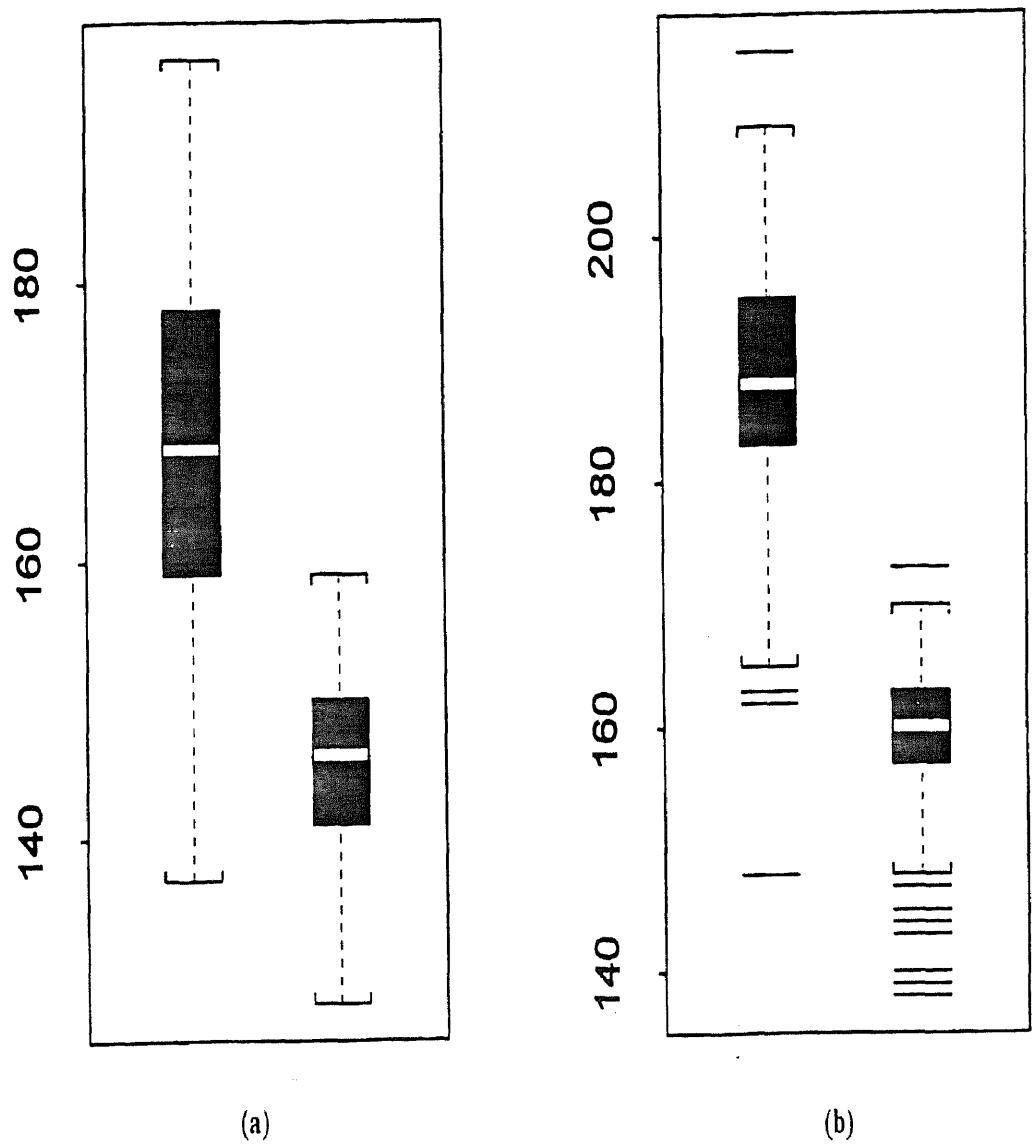

Figure 3.2 Box plots of the IBIs of one pair of subjecs for overall test stages a) Non-paced: sitting. b) Non-paced: supine.

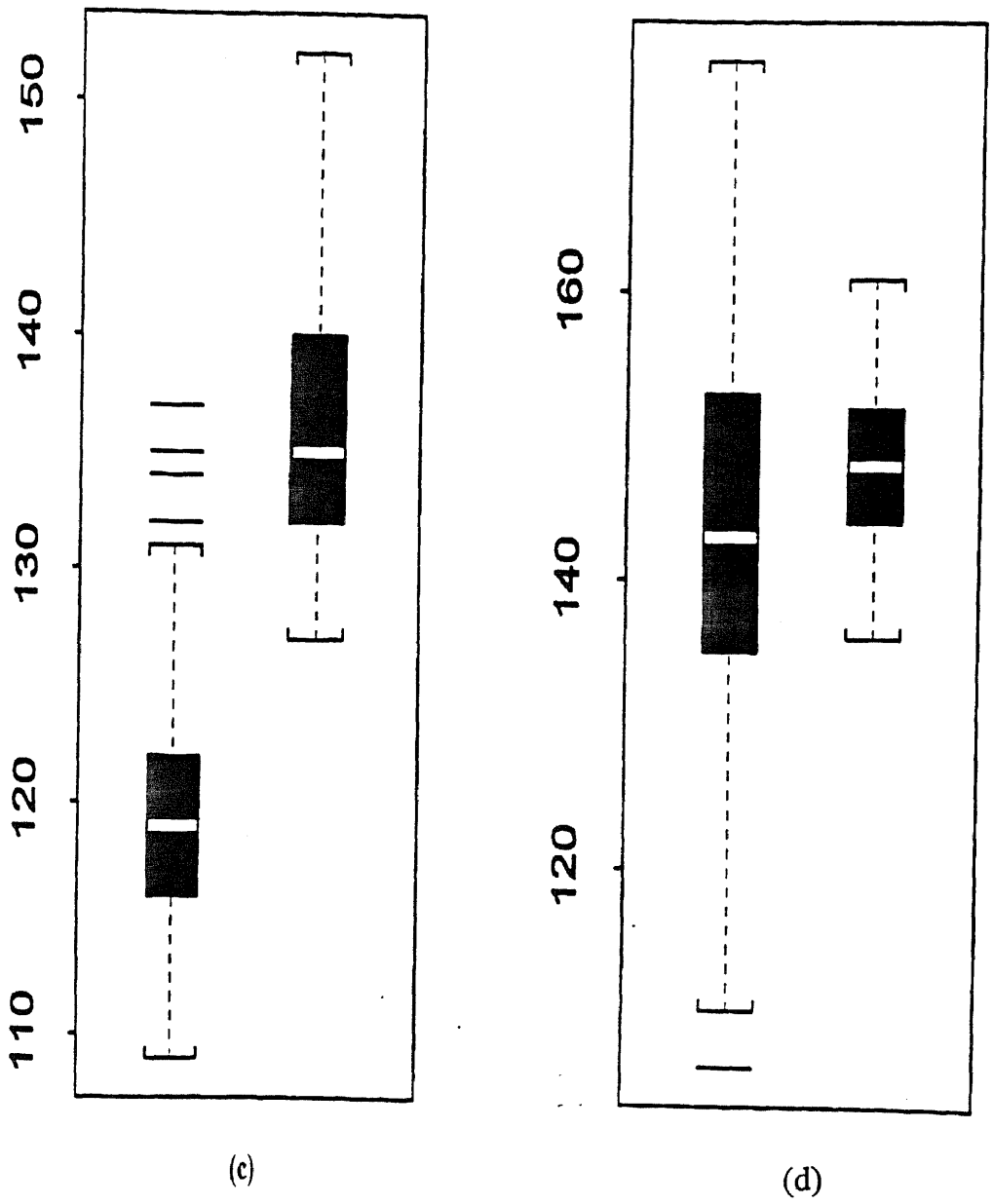

Figure 3.2 Box plots of the IBIs of one pair of subjecs for overall test stages c) Exercise. d) Paced: 8bpm.

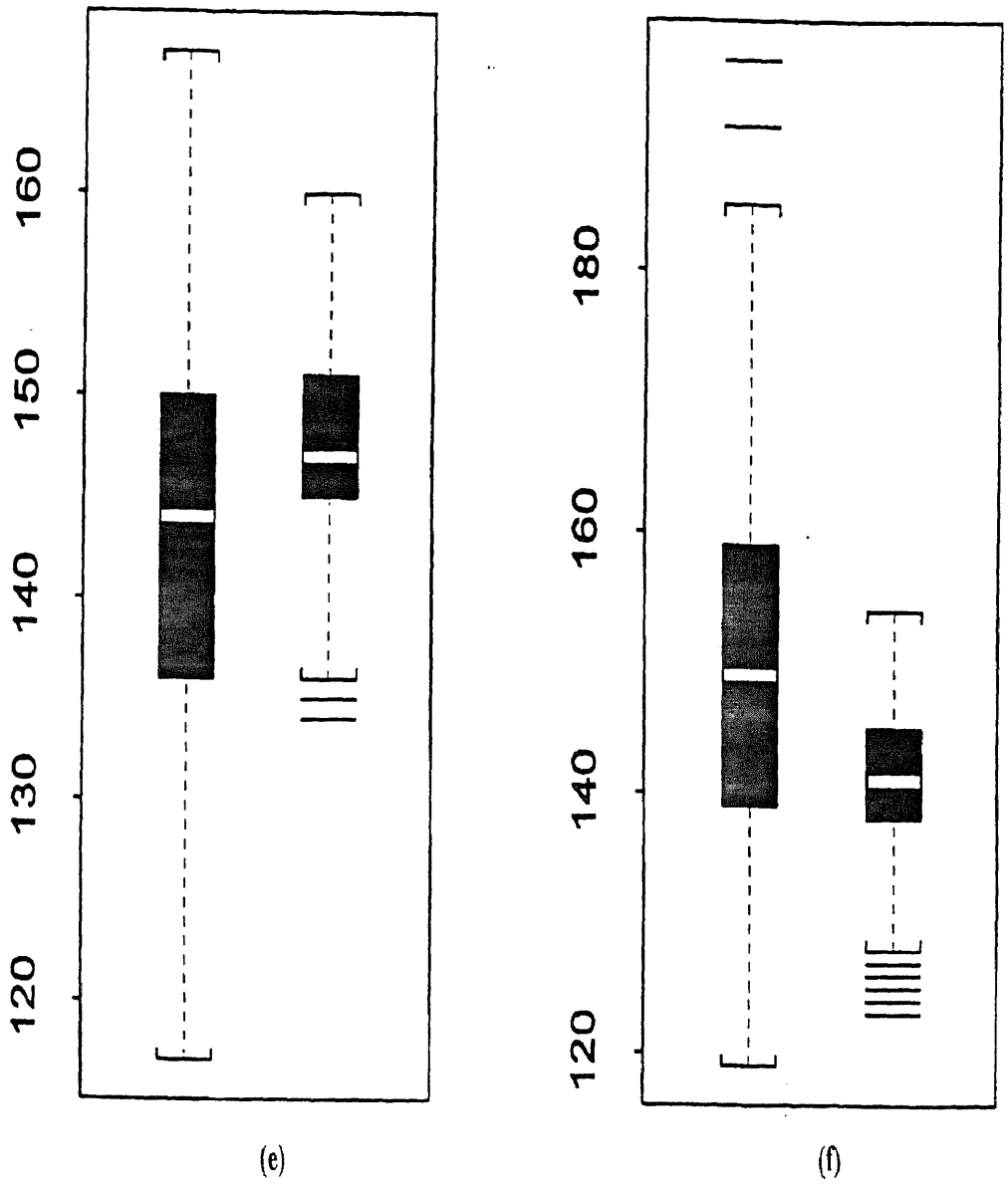

Figure 3.2 Box plots of the IBIs of one pair of subjecs for overall test stages e) Paced 12 bpm. f) Paced: 18bpm

IBI data from stroke survivors. The horizontal line in the interior of each box is located at the median of corresponding IBIs. This estimates the center of the distribution for the data. The height of the box is equal to the inter quartile distance, or IQD, which is the difference between the third quartile of the data and the first quartile. The IQD indicates the spread or width of the distribution for the data. The whiskers (the dotted line extending from the top and bottom of the box) extend to the extreme values of the data or a distance 1.5×IQD from the center, which ever is less. Data points which fall outside the whiskers may be outliers, and so they are indicated by horizontal lines.

Compared with boxes used to represent normal subject's IBIs, the dominant characteristic of the boxes used to represent stroke survivor's IBIs is that they are relatively short for all stages except exercise. This observation indicates that ,with exception of exercise, HRV is larger in normal people than in stroke survivors during all stages. During exercise, since vagal tone of both normal and stroke survivors drops to very low level, it is difficult to compare them.

In order to further compare HRV of normal subjects with that of stroke survivors, IBIs calculated from stage 4 (breathing at 8 min while sitting) for 6 pair of subjects are shown in Figure 3.3. As in Figure 3.2, the boxes on the left side of each graph represent normal subject's IBIs and the boxes on the right side represent stroke survivor's IBIs.

It is clear that the boxes used to represent stroke survivor's IBIs are relative short. This indicates that overall heart rate variability is larger in normal people than in stroke survivors during this stage.

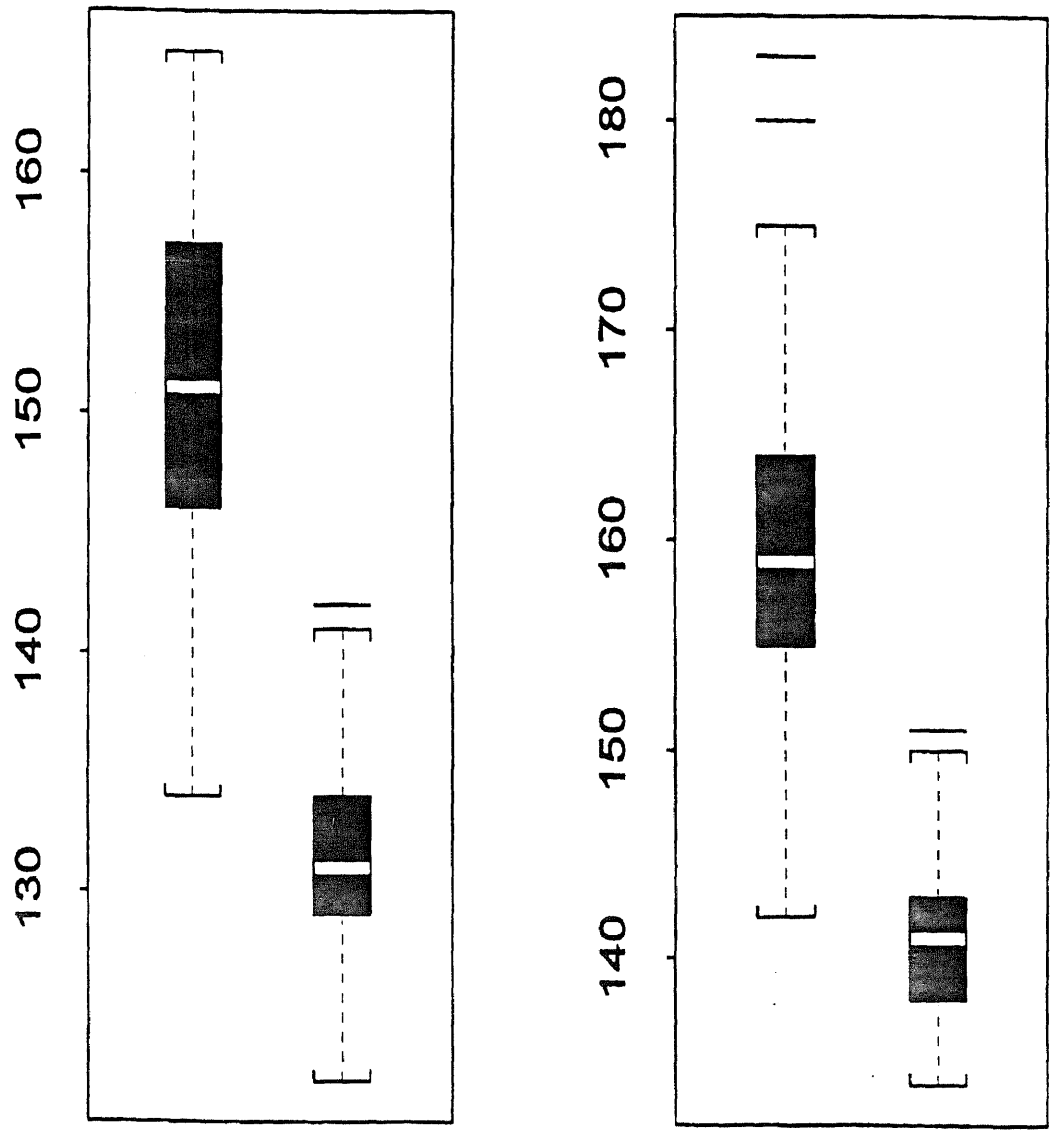

Figure 3.3 Box plots of IBIs of 6 pairs of subjects for 8bpm paced breathing test (a) Pair a. (b) Pair b

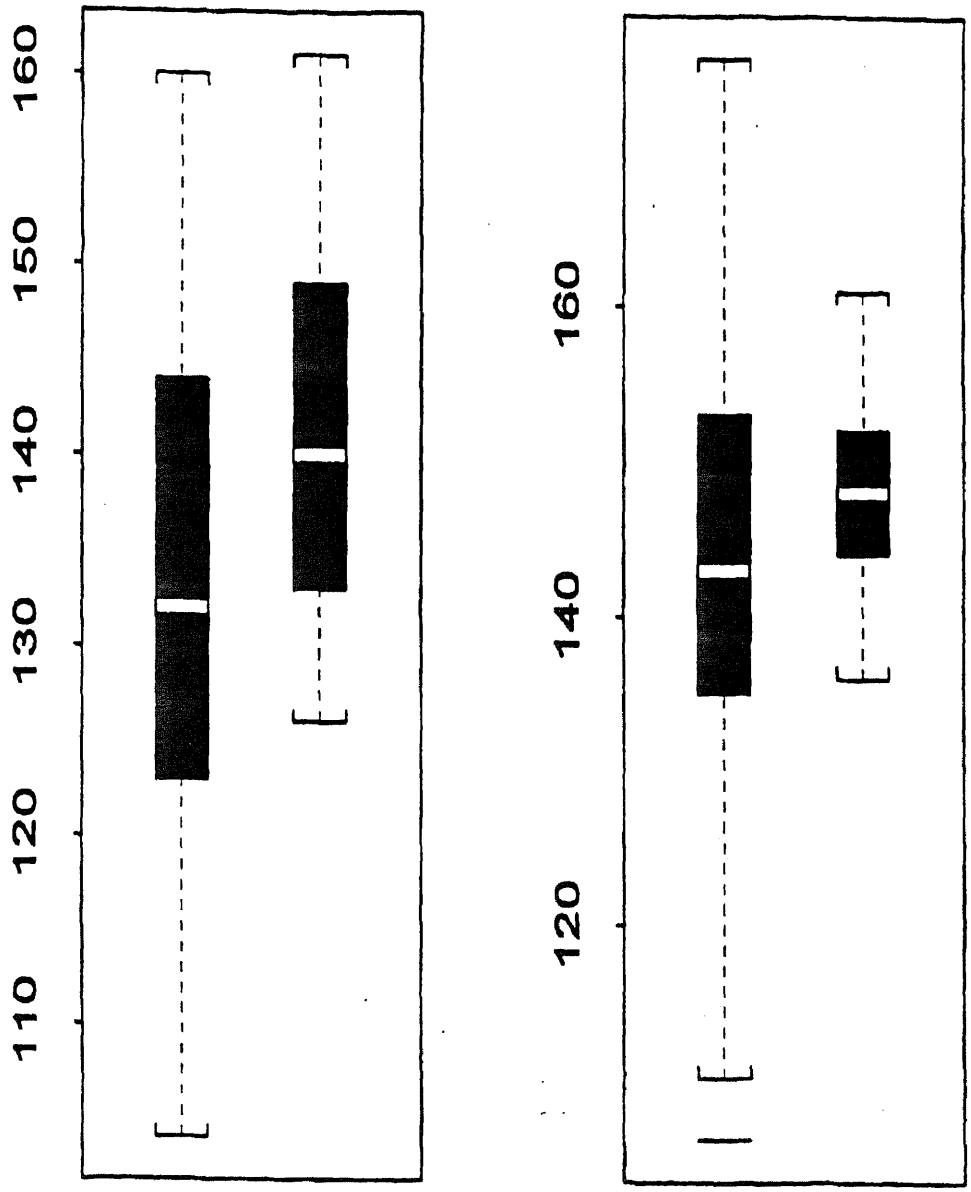

Figure 3.3 Box plots of IBIs of 6 pairs of subjects for 8bpm paced breathing test. (c) Pair c. (d) Pair d.

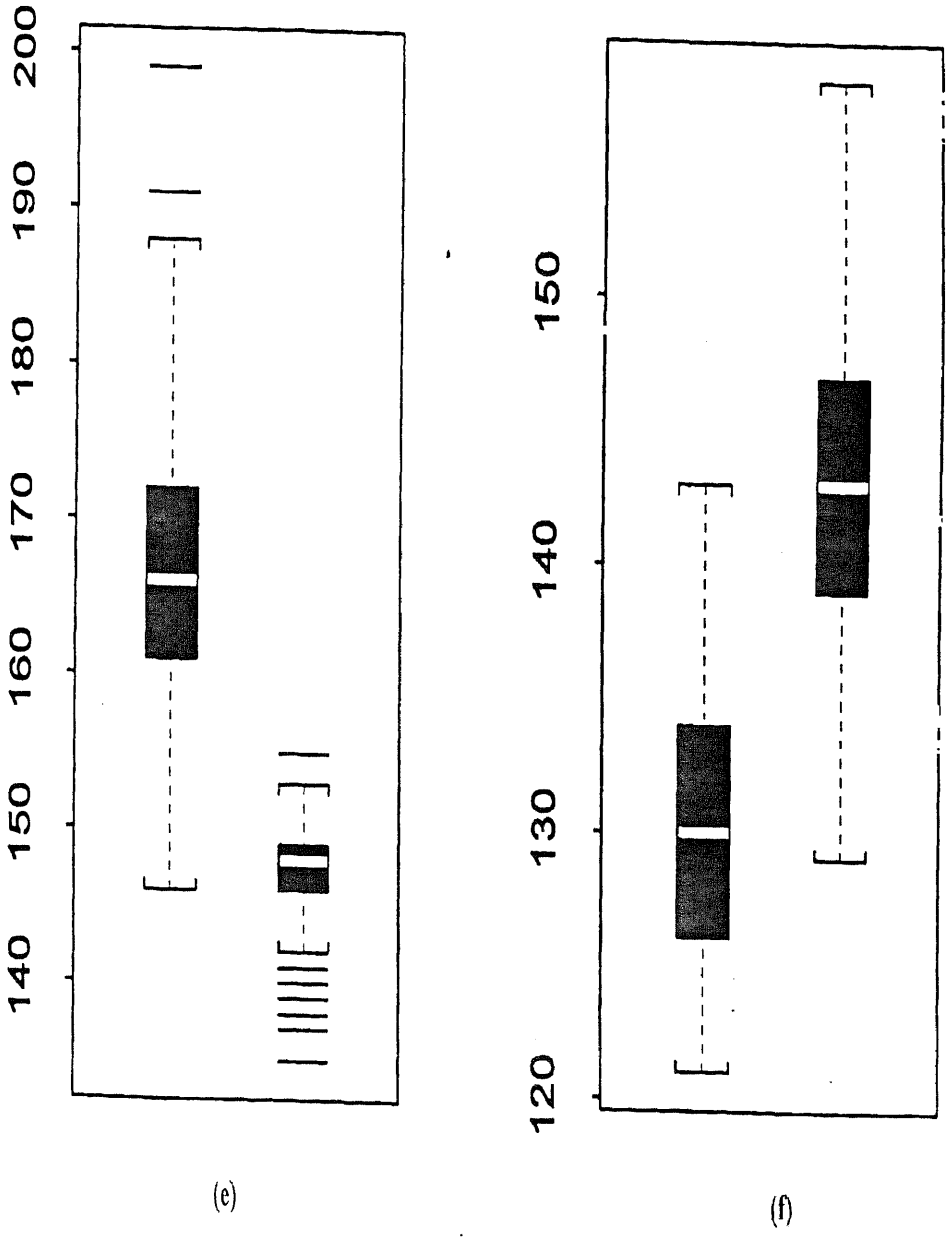

Figure 3.3 Box plots of IBIs of 6 pairs of subjects for 8bpm paced breathing test e) Pair 5. f) Pair 6

3.2 Result of Oral Presentation Test

In the oral presentation test, areas under three major peaks were calculated in the power spectra of HRV for every subject over all tests. As stated in section 1.2 these three major peaks were: the very low frequency peak (0.0033 Hz to 0.04 Hz), the low frequency peak (0.04 Hz to 0.15 Hz) and the high frequency peak (0.15 Hz to 0.4 Hz).

Figure 3.4 shows a typical power spectrum of HRV from a subject, who presented with audience. The X-axis reflects the frequency (Hz), the Y-axis reflects the power density and the shaded part represents the area calculated. The calculated area values from different frequency ranges are presented in Table 3.2, 3.3 and 3.4. The LF:HF ratio values are presented in Table 3.5.

Repeated measures analysis of variance (RANOA) was performed over all testing conditions. The overall effect was significant ($p=0.004$). The post-hoc testing demonstrated significant differences between the high frequency spectral area of the presentation with audience and that of the presentation without audience ($p<0.02$). In addition, significant differences in high frequency power spectra were noted between the anticipatory resting phase and the presentation without audience ($p<0.03$). No significant differences were detected between any of the conditions for low frequency and LF:HF ratio which has been reported to provide information about sympatho-vagal balance [12]

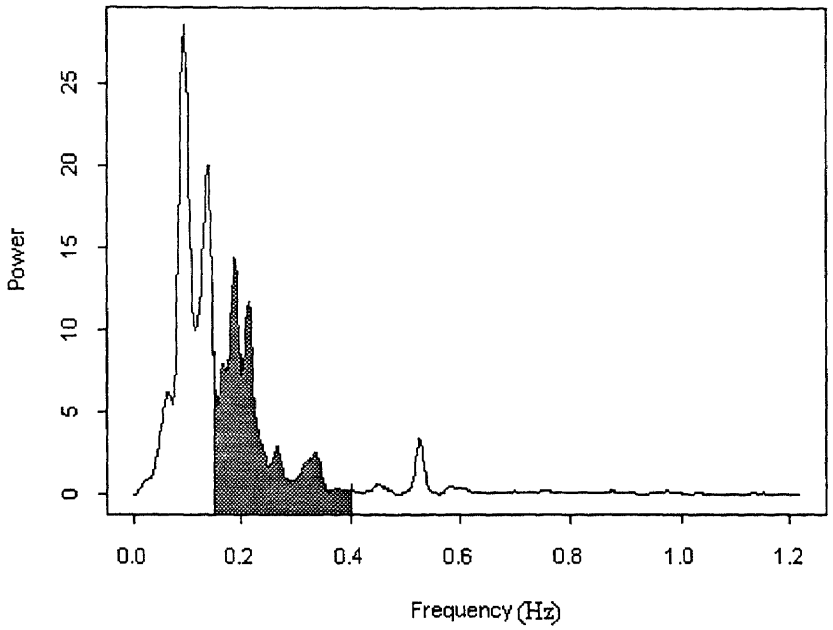

(a)

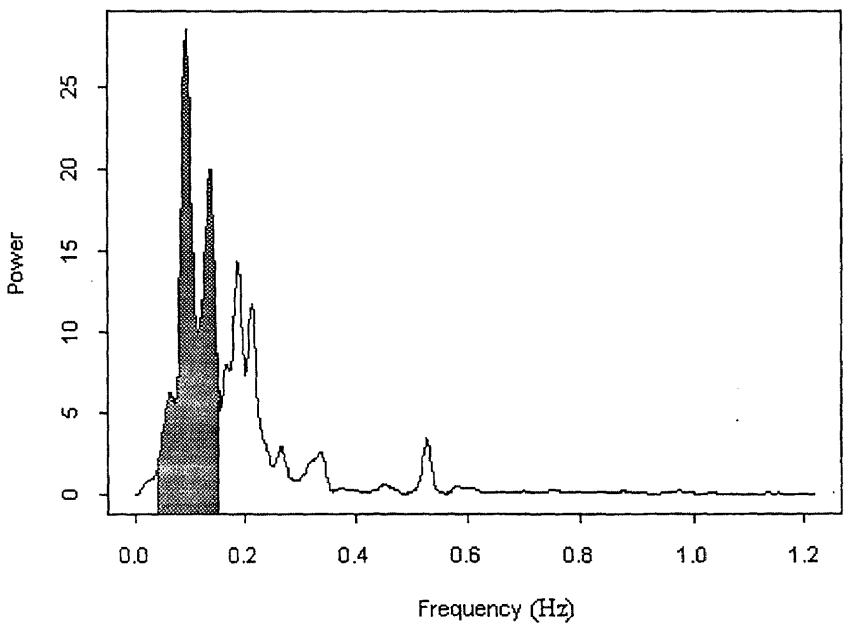

(b)

Figure 3.4 Aeras to be calculated (a) High frequency area. (b) Low frequency area.

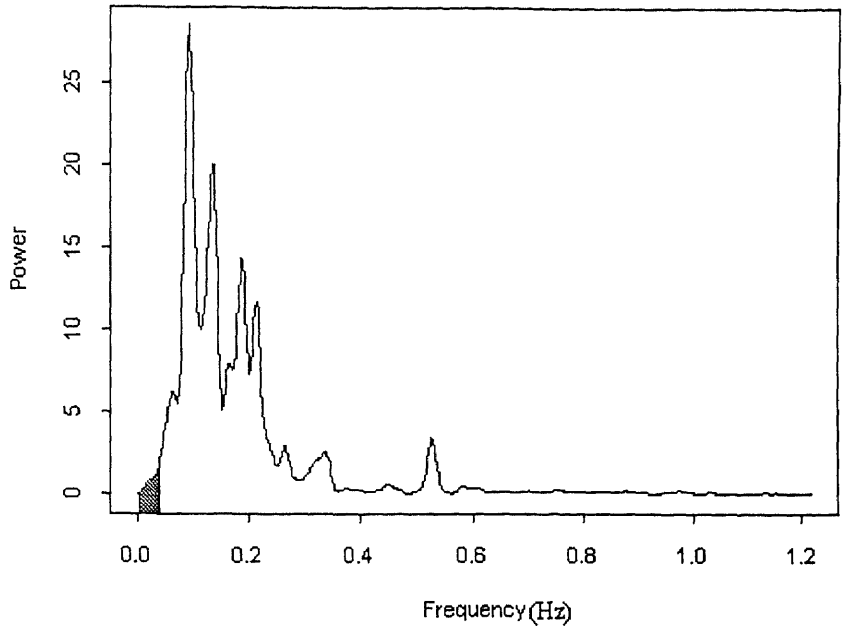

(c)

Figure 3.4 Areas to be calculated. (c) very low frequency.

Table 3.2 High frequency (0.15 Hz to 0.4 Hz) area values

Subject	Anticipiatory resting phase	Presentation with audience	Presentation without audience
1	4.428	2.963	13.474
2	33.456	20.512	13.683
3	1.762	2.709	2.941
4	**	5.167	4.03
5	6.974	1.772	12.218
6	5.432	0.698	5.319
7	4.122	2.87	2.74

Table 3.3 Low frequency (0.04 Hz to 0.15 Hz) area values

Subject	Anticipiatory resting phase	Presentation with audience	Presentation without audience
1	3.695	4.949	21.761
2	63.225	62.194	70.385
3	7.697	16.676	18.239
4	**	25.27	22.896
5	21.297	7.187	26.933
6	14.851	4.138	6.811
7	8.66	3.224	9.977

Table 3.4 Very low frequency (0.0033 Hz to 0.04 Hz) area values

Subject	Anticipiatory resting phase	Presentation with audience	Presentation without audience
1	0.089	0.05	0.408
2	2.155	1.152	3.278
3	0.437	2.027	1.02
4	**	2.028	3.803
5	0.261	0.654	0.755
6	0.538	0.451	0.375
7	0.668	0.348	0.424

Table 3.5 LF:HF ratio values

Subject	Anticipatory resting phase	Presentation with audience	Presentation without audience
1	0.8954	1.67	1.615
2	1.889	3.032	5.144
3	4.368	6.156	6.2
4	**	4.892	5.681
5	3.054	4.056	2.204
6	2.734	5.928	1.281
7	2.1	1.13	3.639

3.3 Cross Correlation of EKG-derived Respiration With Directly Measured Respiration

After developing the EKG-derived respiration method, Zhao and Reisman[13] tested the similarity of the derived respiration spectra to the original respiration spectra by performing a paired t-test and correlation test on the central frequencies for all tests from all subjects and on each individual test for all subjects. As already discussed in section 1.3, the central frequency was formed by first detecting the spectral peak, then the frequency values at 30% of the spectral peak were located on both sides. The two located points were labeled as fl and fh respectively. The central frequency fc was computed so that the area under the spectral curve between fl and fc was equal to the area between fc and fh.

Zhao and Reisman collected data from two lead EKG signals (lead I and III) on 9 healthy subjects during resting, paced breathing (at 8, 12 and 18 breaths per minute), exercise (at 2, 3, 4 times resting metabolic rate), and recovery. The p values from their paired t-test indicated that there is no difference between the mean of the derived central frequency and the mean of the original central frequency. Furthermore, the overall correlation coefficient they calculated was 0.9977, and the correlation coefficient for each individual test varied from 0.8241 to 0.9983. Both paired t-test and correlation test indicated a strong association between the derived central frequency fcd and the original central frequency fco.

However, considering that examination of central frequency only took the main peak of the spectrum into account, it was suggested to further test the total similarity of the derived respiration signal and its spectrum to the original respiration signal and its spectrum using cross correlation methods. In this study, the cross correlation of the derived respiration signal and the original respiration signal, as well as the cross correlation of their spectra were performed.

3.3.1 Understanding of the Cross Correlation

In signal processing, the correlation of two continuous functions f (x) and g (x), denoted as f (x) ∘ g (x), is defined by the relation[27]

$$f(x) \circ g(x) = \int_{-\infty}^{\infty} f(x)^* g(x+a)da \tag{3.1}$$

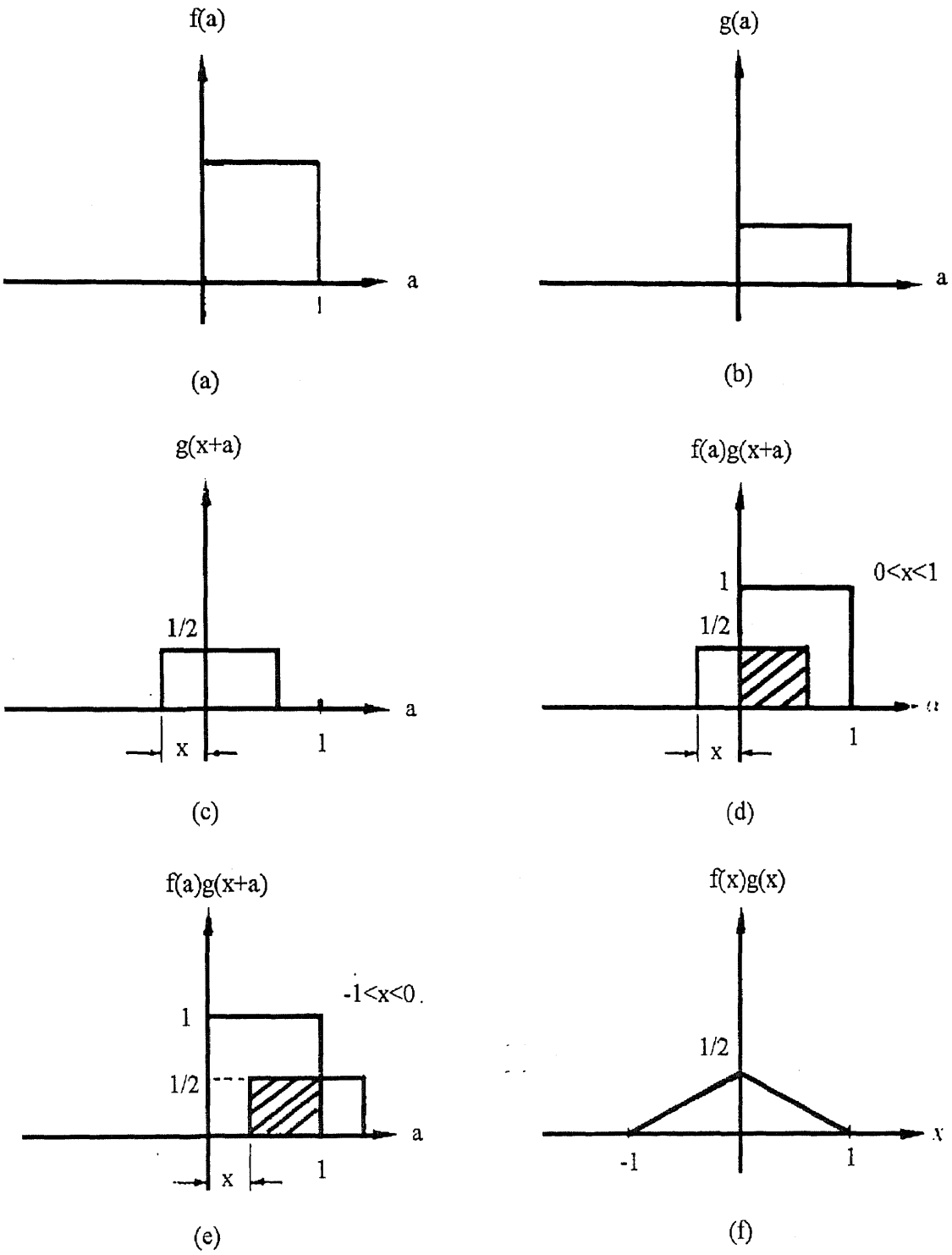

Figure 3.5 Graphic illustration of correlation. The shaded areas indicate regions where the product is not zero.

where * is the complex conjugate. We slide g (x) by f (x) and integrate the product from $-\infty$ to ∞ for each value of displacement x. Figure 3.5 illustrates the procedure to perform the correlation calculation. In Figure 3.5 (a) and (b), two continuous functions f (x) and g (x) are shown as square and rectangle functions respectively. Figure 3.5 (d) represents g (x) being slid to the left hand side of f (x) where $0 \le x \le 1$. (e) represents g(x) being slid to the right hand side of f (x) where $-1 \le x \le 0$ and (f) represents the correlation of f (x)$\circ$g (x). The shaded areas indicate regions where the product is not zero. It is clear that the cross correlation of two continuous function is a continuous time series. The cross correlation at zero lag represents the situation when two signals are superimposed on each other without any shifting. If the cross correlation function is normalized by $\sqrt{autc(f(x))} * \sqrt{autc(g(x))}$,where autc represents the auto cross correlation, then the normalized cross correlation at zero lag would be 1.0 when the two signals are exactly the same, and less than one for less similar signals.

In order to further understand the meaning of cross correlation, the cross correlation was performed on two sine waves under different conditions: (1) two identical sine waves, which contain the same frequencies, phases and amplitudes. f(t)=$\sin\omega_1 t$, g(t)=$\sin\omega_2 t$, where $\omega_1 = \omega_2$; (2) two sine waves with different frequencies. f(t)= $\sin\omega_1 t$, g(t)= $\sin\omega_2 t$, where $\omega_1 \neq \omega_2$, and ω_1, ω_2 are not multiples of each other. (3) one sine wave contained in the other sine wave. f(t)= $\sin\omega_1 t + \sin\omega_2 t$, g(t)= $\sin\omega_1 t$; (4) both sine waves with the same frequencies, but 180° out of phase to each other; and (5) both sine waves contain DC values. f(t)=1+$\sin\omega_1 t$, g(t)=1+$\sin\omega_2 t$, where $\omega_1 = \omega_2$. Figures 3.6 to 3.10 demonstrate

the cross correlation under all different conditions mentioned above, respectively. In the figures, the x axis represents the index number and the y axis represents the signal values. In Figure 3.6, since the two sine waves represented in (a) and (b) contain same frequencies, phases and amplitudes, the cross correlation at zero lag is equal to 1. This demonstrates the situation that the normalized cross correlation at zero lag is 1.0, when two signals are exactly the same. In this example, the reason that the normalized cross correlation is less than 1 at peaks other than at zero lag is because that g(t) has the same length as f(t). If the length of g(t) were three or more times the length of f(t), then the normalized cross correlation would be equal to 1 at peaks other than at zero lag. The situation that the normalized correlation at zero lag is less than one is demonstrated in Figure 3.7. The two sine waves represented in 3.7(a) and (b) contain different frequencies. The frequency of one sine wave is much higher than that of the other, and the frequency of one sine wave is not a multiple of the frequency of the other sine wave. The cross correlation of these two signals at zero lag is 0.0438, which is much less than 1. Figure 3.8 demonstrates the situation in which one signal is contained in the other. The cross correlation of the signals $\sin\omega_1 t$ and $\sin\omega_1 t + \sin\omega_2 t$ at zero lag is 0.7054, which is less than 1, but much higher than 0.0438. The three examples mentioned above imply that the higher the cross correlation at zero lag the more the two signals are similar to each other. If one signal is a "component" of the other signal, the cross correlation of these two signals at zero lag is higher than the cross correlation at zero lag of two totally different signals, but lower than that of two identical signals. It is easy to deduce that if this frequency "component"

becomes bigger and bigger, the cross correlation at zero lag will become more and more close to 1. But what happens when two signals contain the same frequencies but are 180° out of phase. This question is answered in Figure 3.9. In this situation, the cross correlation at zero lag becomes -1. This example indicates the meaning of -1 in the cross correlation. Figure 3.10 demonstrates another situation when both signals contain DC component. In this case, there is no negative value existing in the cross correlation series and the shape of cross correlation wave of the two signals containing a DC component is different from the shape of the cross correlation wave of the two same signals without DC component. This is shown in following deduction.

Suppose the length of f(x) and g(x) is $2l$, the cross correlation of 1+f(t) and 1+g(t) is as follow:

$$
\begin{aligned}
[1+f(t)]\circ[1+g(t)] &= \int_{-l}^{l}[1+f(t)][1+g(t+a)]da \\
&= \int_{-l}^{l}[1+g(t+a)+f(t)+f(t)g(t+a)]da \\
&= \int_{-l}^{l} f(t)g(t+a)da + 2l + 2lf(t) + \int_{-l}^{l} g(t+a)da \qquad (3.2)
\end{aligned}
$$

The outcome of the above equation, which shows the cross correlation of two signals containing DC components, has a different outcome from that of Eq.(3.1) due to the resulting cross products $(2lf(t), \int_{-l}^{l} g(t+a)da)$. As shown in

Figures 3.6 and 3.10, the DC shift changes the outcome of cross correlation. This implies that it is better to remove the DC component from the signals before performing the cross correlation.

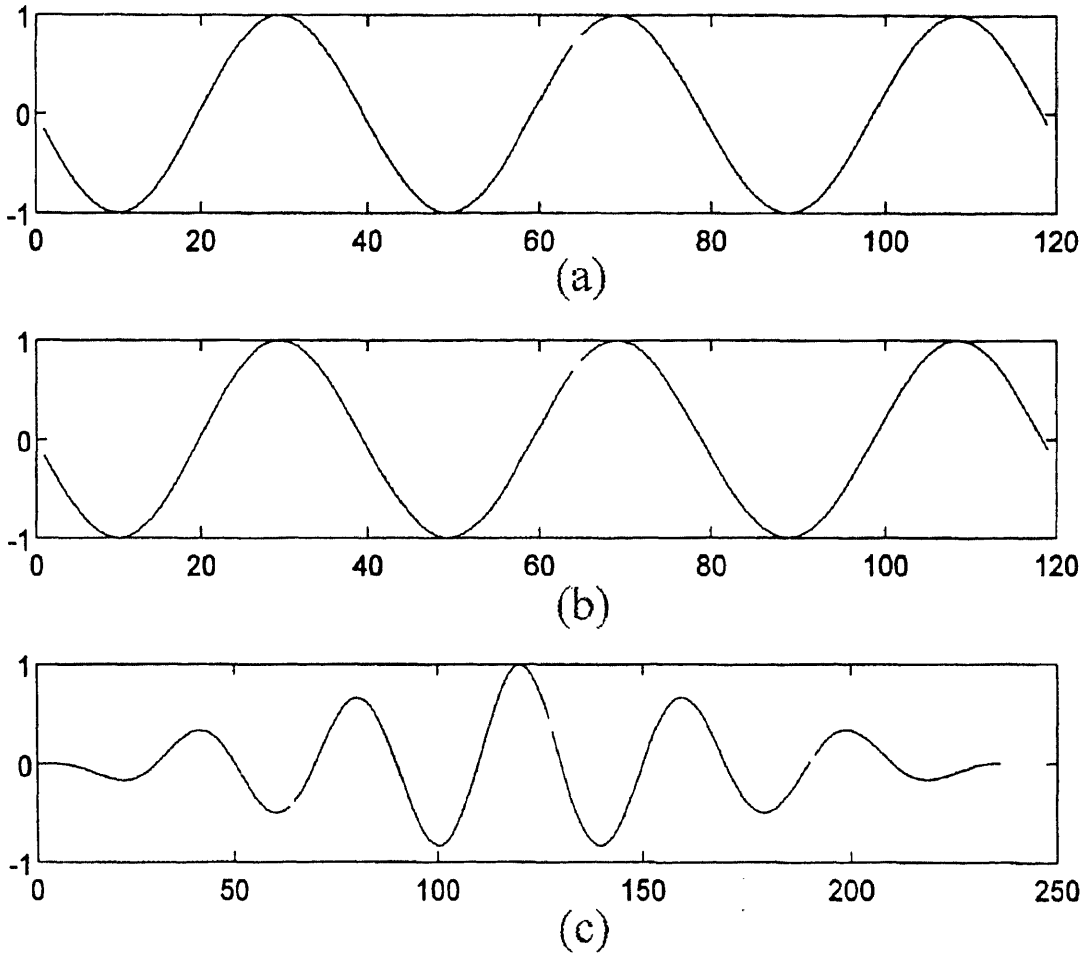

Figure 3.6 Cross correlation of two same sine waves. (a) $\sin \omega_1$; (b) $\sin \omega_2$; (c) $\sin \omega_1 \circ \sin \omega_2$ $(\omega_1 = \omega_2)$

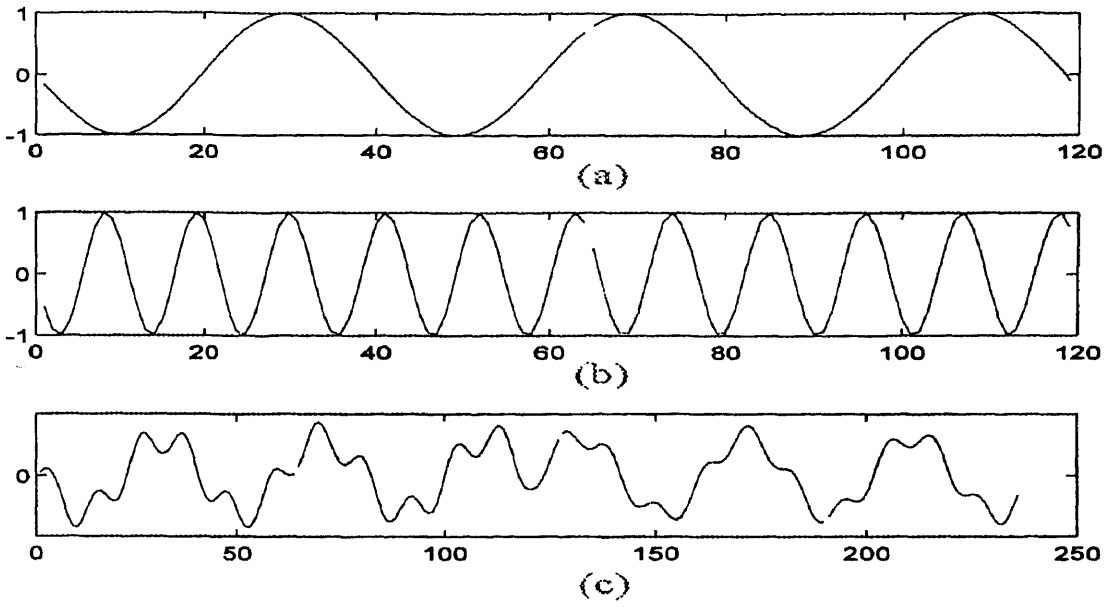

Figure 3.7 Cross correlation of two different sine waves. (a) $\sin \omega_1$; (b) $\sin \omega_2$; (c) $\sin \omega_1 \circ \sin \omega_2$ $(\omega_1 \neq \omega_2)$

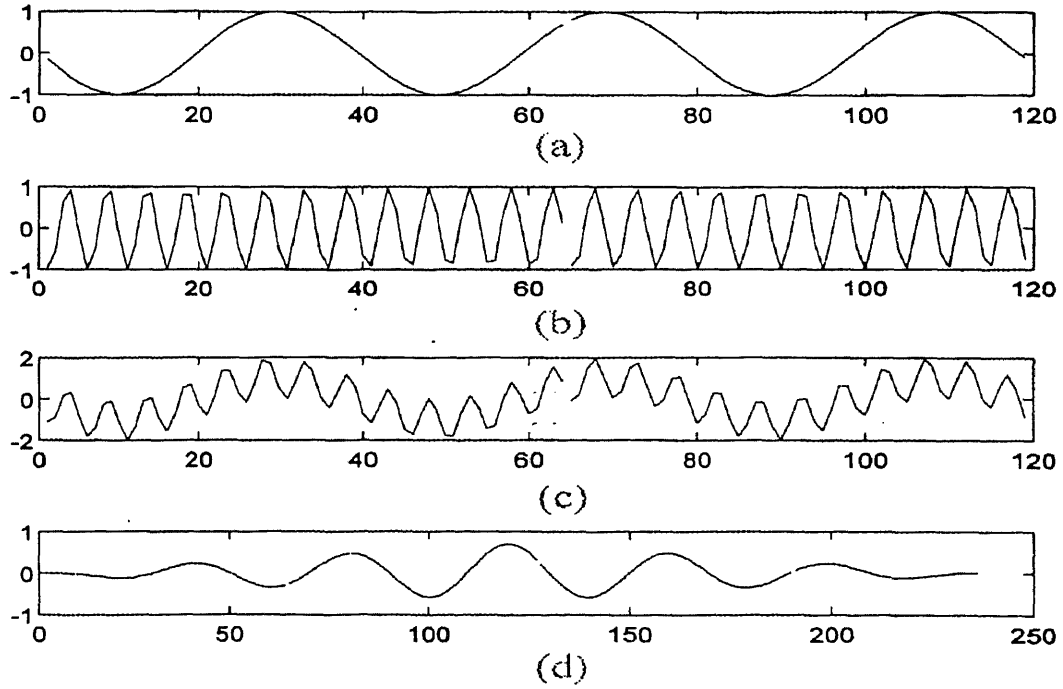

Figure 3.8 Cross correlation of two sine waves, one sine wave is contained in the other. (a) $\sin \omega_1$. (b) $\sin \omega_2$. (c) $\sin \omega_1 + \sin \omega_2$. (d) $\sin \omega_1 \circ (\sin \omega_1 + \sin \omega_2)$.

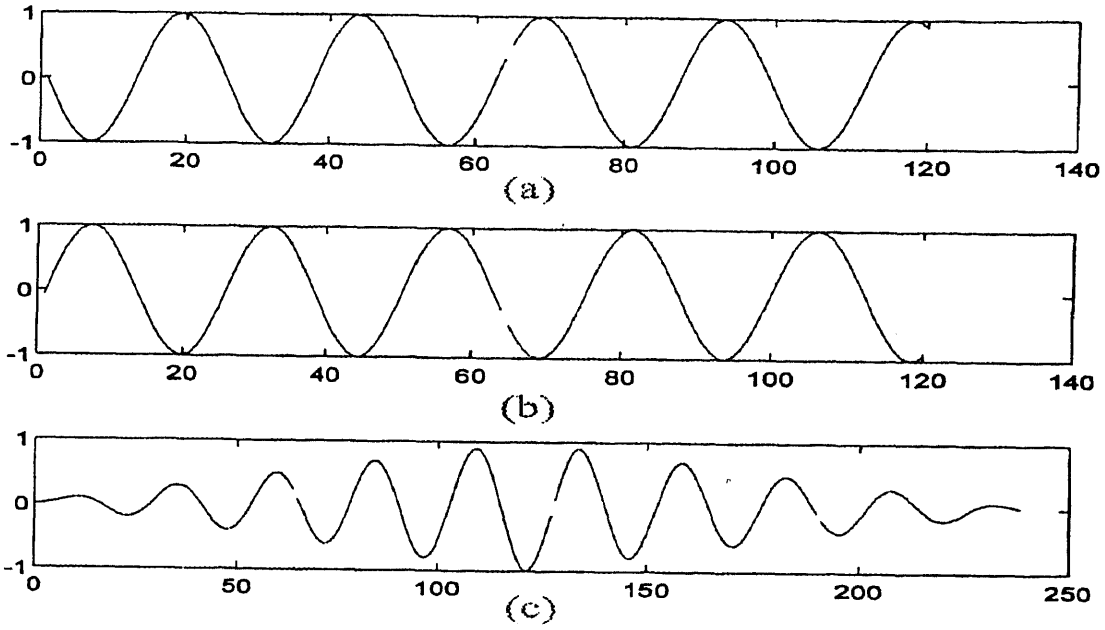

Figure 3.9 Cross correlation of two sine waves which are 180° out of the phase. (a) $\sin\omega t$. (b) $\sin(\omega t+\pi)$. (c) $\sin\omega t \circ \sin(\omega t+\pi)$

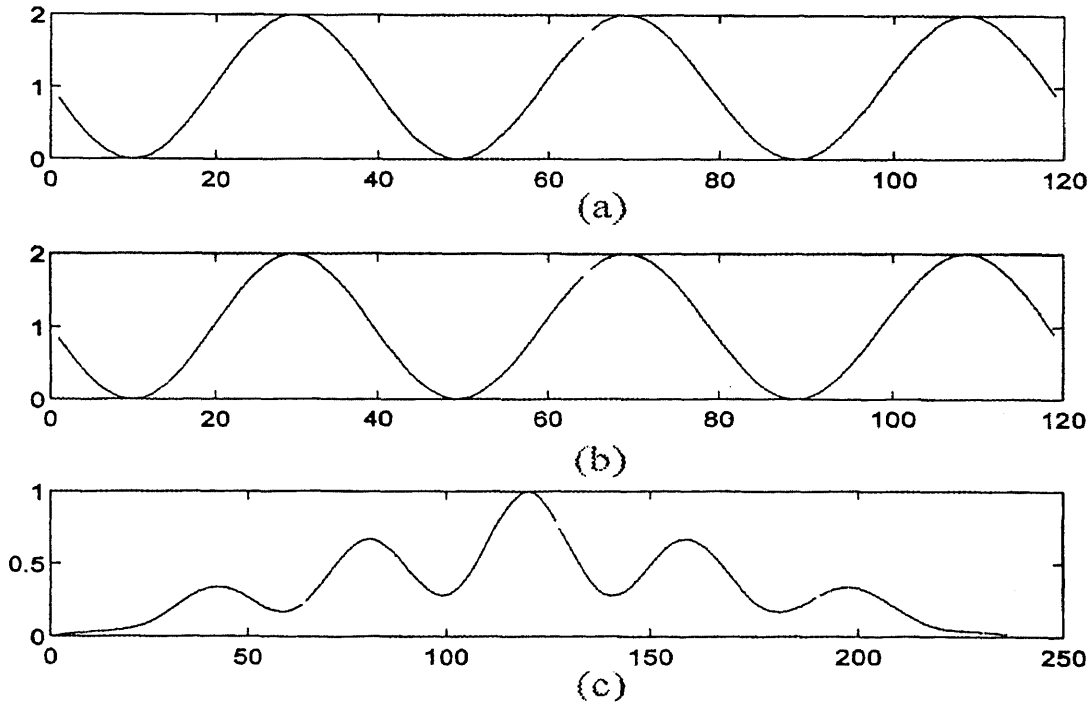

Figure 3.10 Cross correlation of two sine waves which contain DC component. (a) $\sin\omega t+1$. (b) $\sin\omega t+1$. (c) $(\sin\omega t+1)\circ(\sin\omega t+1)$

3.3.2 Cross Correlation of EKG Derived Respiration with Original Respiration

Based on the understanding of cross correlation shown in section 3.3.1, we performed cross correlation on the derived respiration and the corresponding original respiration. For the respiration time domain signals of 8 subjects obtained by Zhao and Reisman, the maximum cross correlation for each individual test are displayed in Table 3.6 and for the respiration spectrum (frequency domain) data of 8 subjects obtained by Zhao and Reisman, the maximum cross correlations for each individual test are displayed in Table 3.7. Figure 3.11 and Figure 3.12 demonstrate an example of the cross correlation of a derived respiration signal with an original respiration as well as the cross correlation of the spectrum of a derived respiration with the spectrum of an original respiration, respectively.

Table 3.6 Cross correlations of EKG-derived respiration signals and original respiration signals (Missing values are marked with asterisk) (Time domain)

Subject	rest	8bpm	12bpm	18bpm	2 mets	3 mets	4 mets	recovery
1	0.839	0.903	0.916	0.958	0.807	0.856	0.921	0.756
2	0.993	0.954	0.974	0.988	0.974	0.936	0.941	0.969
3	0.988	0.947	0.989	0.958	0.658	0.760	0.325	0.653
4	0.992	**	0.993	**	0.949	**	**	0.972
5	0.985	0.952	0.986	0.992	0.963	0.938	0.864	0.919
6	0.969	0.945	0.965	0.972	0.958	0.936	0.960	0.959
7	0.89	0.828	0.954	0.946	0.686	0.619	0.769	0.853
8	0.992	0.926	0.951	0.967	0.976	0.962	0.957	0.996

Table 3.7 Cross correlation of EKG-derived respiration spectra and original respiration spectra (Missing values are marked with asterisk)(Frequency domain)

Subject	rest	8bpm	12bpm	18bpm	2 mets	3 mets	4 mets	recovery
1	0.988	0.990	0.844	0.973	0.914	0.977	0.982	0.967
2	0.983	0.952	0.945	0.996	0.992	0.371	0.903	0.958
3	0.919	0.639	0.916	0.833	0.828	0.749	0.204	0.825
4	0.876	**	0.781	**	0.880	**	**	0.928
5	0.769	0.576	0.844	0.822	0.317	0.941	0.748	0.910
6	0.991	0.998	0.997	0.997	0.758	0.994	0.954	0.979
7	0.914	0.998	0.997	0.971	0.295	0.451	0.875	0.995
8	0.865	0.998	0.993	0.994	0.896	0.778	0.825	0.859

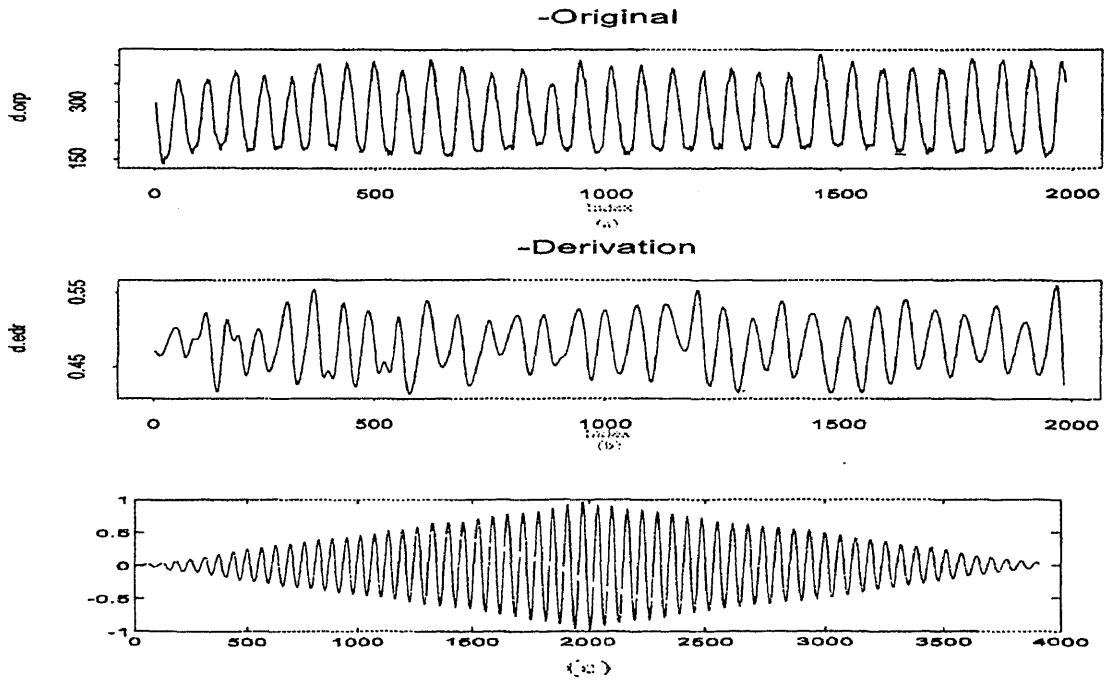

Figure 3.11 Cross correlation of the EKG derived respiration with the original respiration. (a) Original respiration. (b) EKG derived respiration. (c) The cross correlation of the original respiration and the EKG derived respiration.

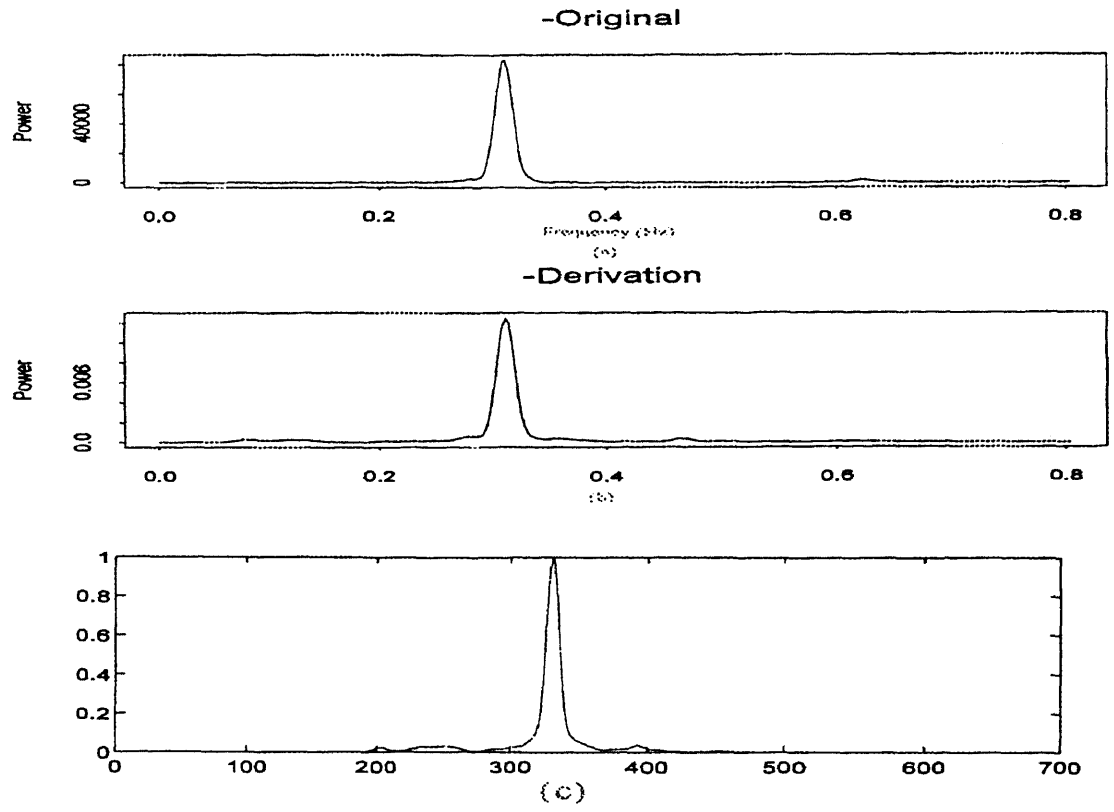

Figure 3.12 Cross correlation of the spectrum of the EKG derived respiration with the spectrum of the original respiration. (a) The spectrum of the original respiration. (b) The spectrum of the EKG derived respiration. (c) The cross correlation of the spectrum of the original respiration with the spectrum of the EKG derived respiration.

From table 3.6 and 3.7, it is observed that, in most cases, the derived respiration strongly correlates with the original respiration both in time and frequency domain. However, in some cases, cross correlation drops to low values. One of these situations is demonstrated in Figure 3.13. where the cross correlation of the original respiration with the EKG derived respiration at zero lag is only equal to 0.325. The reason causing such a low cross correlation between two signals is that the original respiration signal has a very low signal to noise ratio.

Another factor leading to incidence of low cross correlation is as follow: The EKG-derived respiration technique is based on the phenomenon that respiration modulates the change in the angle of the cardiac electrical vector axis. This modulation is subject dependent, some having large modulation, while others having small modulation. It might be related to the type of respiration (abdominal versus thoracic) and the difference in the anatomical structure of each individual, or it might be related to tidal volume. The correct respiration might not be derived reliably if the EKG signal is poorly recorded or has a very low signal to noise ratio. The changes in the angle of the cardiac electrical vector are also influenced by sources besides respiration. For instance, during intense body movement (e.g. Figure 3.13), the respiration signal might not be correctly obtained from the EKG signal.

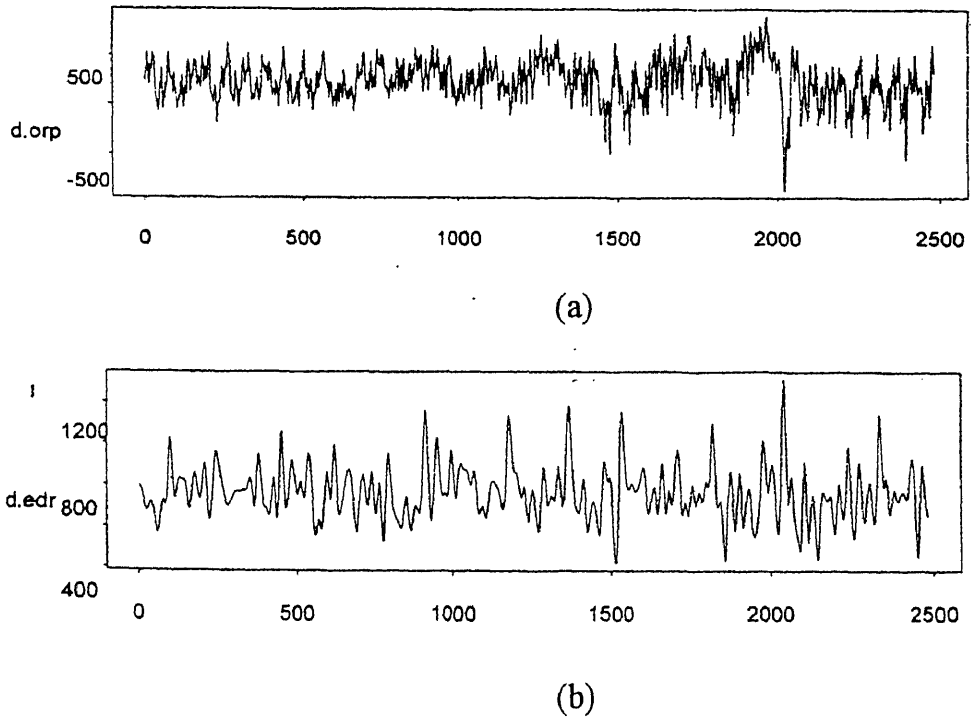

Figure 3.13 Respiration signals which cause low cross correlation. (a) Original respiration. (b) EKG derived respiration.

Therefore, besides reducing the intense body movement, methods to improve EKG derived respiration must be further investigated, and may include improving the EKG derived respiration technique as well as finding more suitable electrode positions.

3.4 Fidelity of Holter Recorder Playback System

In order to evaluate the fidelity of the Holter recorder playback system, a simulated EKG signal was compared with the same EKG signal recorded with a Holter recorder. A five-minute 60 beats per minute EKG signal generated by the Quinton Q4000 Stress Test Monitor/Controller (Quinton Instrument, Co., Seattle, WA) was acquired directly into the IBM compatible 386 data acquisition computer at a sampling rate of 200 Hz and another five-minute 60 beats per minute simulated EKG was next recorded with the Holter recorder. The recorded EKG signal was played back on both a JVC TD W-10 and a Panasonic RX C-38 cassette tape recorder. The output of the two tape recorders were acquired into the same data acquisition computer at an accelerated sampling rate of 9.62 kHz, which corresponds to 200 samples per second in real time. Figure 3.14 (a) illustrates the two consecutive QRS complexes of the original EKG signal. Figure 3.14 (b) illustrates the same signal output from the Panasonic RX C-38 cassette player and (c) illustrates the same signal output from the JVC TD W-10 cassette desk. Comparing Figure (b), (c) with Figure (a), visually we could tell that both output EKGs were distorted. However, the EKG from the Panasonic RX C-38 was distorted more seriously. It contained more noise, and the S waves dropped lower

as compared with the EKG from the JVC TD W-10. The reason for the distortion in the EKGs output from both playback systems is that both systems do not have a low enough frequency response. The Panasonic RX C-38 cassette has a frequency response of 90 Hz to 11000 Hz and the JVC TD W-10 cassette has a frequency response of 30 Hz to 16000 Hz. If all frequency components of EKGs, which are from 0.05 Hz to 100 Hz, recorded by the Holter recorder were output from the tape player, the requirement of the frequency responses of the tape player should be from 2.5 Hz to 5000 Hz, because the play back speed is about 50 times faster than the recording speed. Since the frequency responses of both tape playback systems do not cover the required low frequency range, the low frequency information of the Holter recorded EKGs is lost, and therefore, the signal is distorted. Since the JVC TD W-10 cassette desk covers more low frequency range than the Panasonic RX C-38, the EKGs output from JVC TD W-10 cassette is more similar to the original signal than that from the Panasonic RX C-38.

The cross correlations were performed on the original simulated EKG signal and JVC TD W-10 output EKG signal, as well as on their corresponding spectra. Figure 3.15 shows both simulated and recorded EKG signals and their corresponding spectra. In Figure 3.15 (a), the top graph is the original simulated EKG signal and the bottom graph is the EKG signal output from the JVC TD W-10 cassette player, and both corresponding spectra are shown in Figure 3.15 (b). The cross correlation of simulated and recorded EKG signals is 0.69, and the cross correlation of the spectrums is 0.9859. The reasons of low correlation are discussed fully below

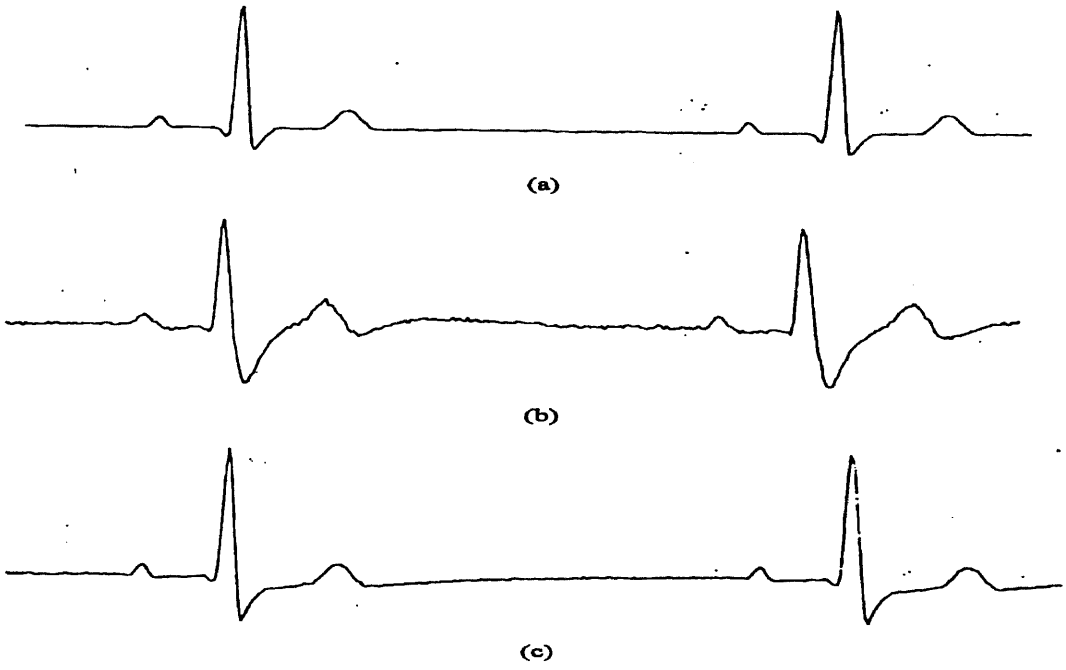

Figure 3.14 Comparison of different play back systems. (a) Original simulated EKG, (b) Simulated EKG output from Panasonic RX C-38 cassette player. (c) Simulated EKG output from JVC TD W-10 cassette desk

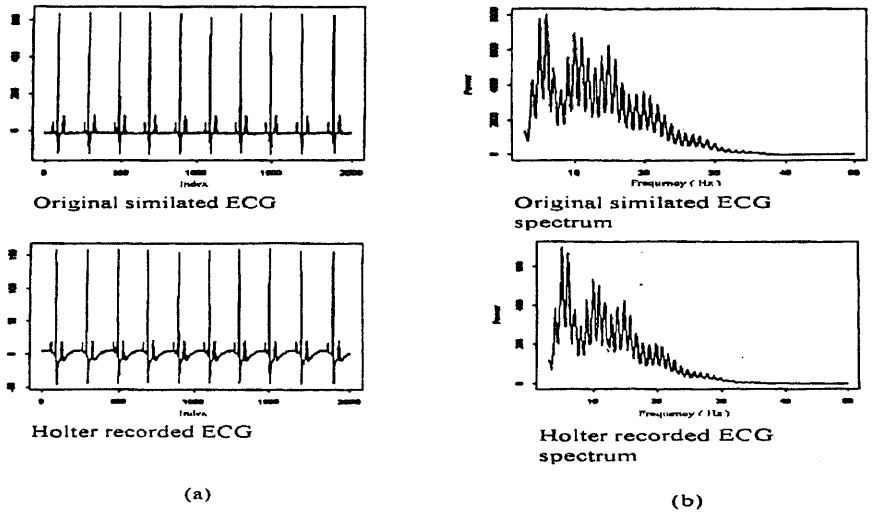

Figure 3.15 Comparison of original and Holter recorded EKG signals and their spectra

3.5 Variables Affecting the Quality of the Holter Data Processing

3.5.1 Speed Variation of Holter System.

Our JVC TD W-10 cassette replayed the EKG tape at 48.1 times the recording speed and the acquisition computer sampled at an accelerated rate of 9.62 kHz, which corresponds to approximately 200 samples per second in real time. In such a setup, even minute variations in speed of either the original recording system or the replaying system may introduce non quantifiable errors in the R-R interval series. The stability of the tape speed of the Holter recorder-cassette playback system was tested by Zhao [20]. In his study, a two minutes 60 beat per minute simulated EKG was next recorded by the Holter recorder, acquired into the data acquisition computer at a sampling rate of 9.62 kHz, and processed in S-Plus. Considering the mean of the interbeat intervals and the interbeat interval with the biggest variation, the relative speed stability of our Holter recorder-cassette playback system reported in his study is 99.08%. In order to ensure recording valid EKG data, the following reminders are provided for optimum performance of the Holter recorder.

1) Before data collection, ensure that the battery is in good working condition.

2) To ensure recording valid EKG data, it is highly recommended that a new tape is for each recording.

3) Emphasize to the patient the importance of accuracy in the patient diary. The patient must note the time, symptoms, and activity taking place when any kind of discomfort (e.g. shortness of chest pain) is experienced.

4) Alert the patient to avoid sources of electrical interference and also to avoid exposing the recorder to water.

3.5.2 Presence of Premature Contractions in the R-R Interval Data

A premature contraction is a contraction of the heart prior to the time that normal contraction would have been expected[1]. Most premature contractions result from ectopic foci in the heart, which emit abnormal impulses at odd times during the cardiac rhythm. Among the possible causes of ectopic foci are (1) local areas of ischemia; (2) small calcified plaques at different points in the heart, which press against the adjacent cardiac muscle so that some of the fibers are irritated; and (3) toxic irritation of the A-V node, Purkinje system, or myocardium caused by drugs, nicotine, or caffeine. In persons with ischemic heart disease, the ectopic rhythm is, on occasion, believed to be caused by a re-entrant signal as follows: The normal heartbeat excites an area of ischemic tissue in which the cardiac impulse travels extremely slowly. Then, after the contraction of the normal heart muscle is over, the slowly traveling signal in the ischemic tissue escapes back into the normal cardiac muscle, in this way causing a second contraction at a later time in the heartbeat. Premature contractions are generated locally, they are not controlled by the autonomic nervous system. The premature contractions not only occur in people whose hearts are not in a healthy condition, but also occur frequently in healthy persons and, indeed, are often found in athletes or others whose hearts are certain to be in healthy condition. Figure 3.16 is an EKG showing a single premature contraction. The QRS complex of this beat occurs too soon in the heart

cycle, and the interval between the premature contraction and the next succeeding contraction is prolonged.

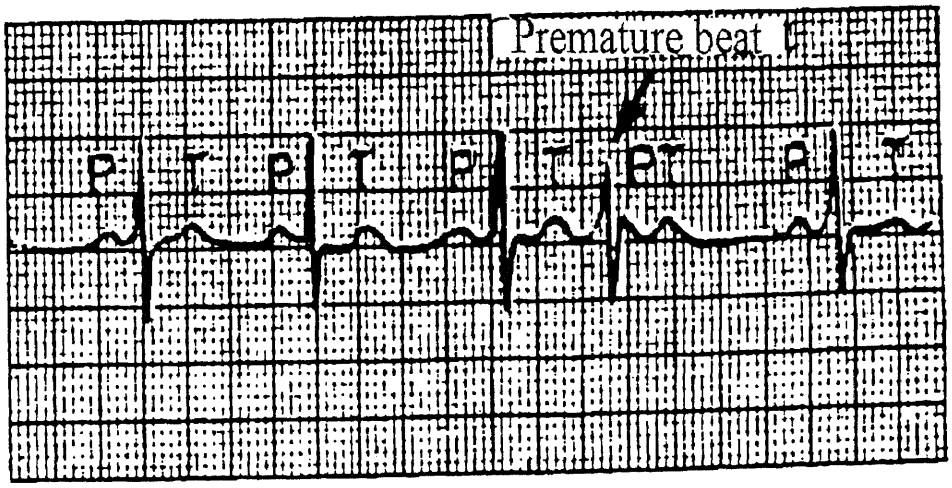

Figure 3.16 Premature contraction

The presence of premature contractions results in an abnormality in the interbeat intervals, which further affects the spectrum of the HRV. Figure 3.17 demonstrates the affect of a premature contraction on the heart rate spectrum[21]. Figure 3.17 (a) shows a heart rate signal containing a premature contraction, which is characterized by a sharp increase followed by a sharp decrease in the rate. (c) shows the spectrum of the heart rate signal displayed in (a). (b) shows the same heart rate signal as which displayed in (a), except that the premature contraction "artifact" is eliminated. (d) shows the spectrum of the heart rate signal displayed in (c). By comparing the spectra of both signals, it is obvious that the spectrum of the

signal containing a premature contraction contains a broad poorly defined peak caused by the spike in the time series.

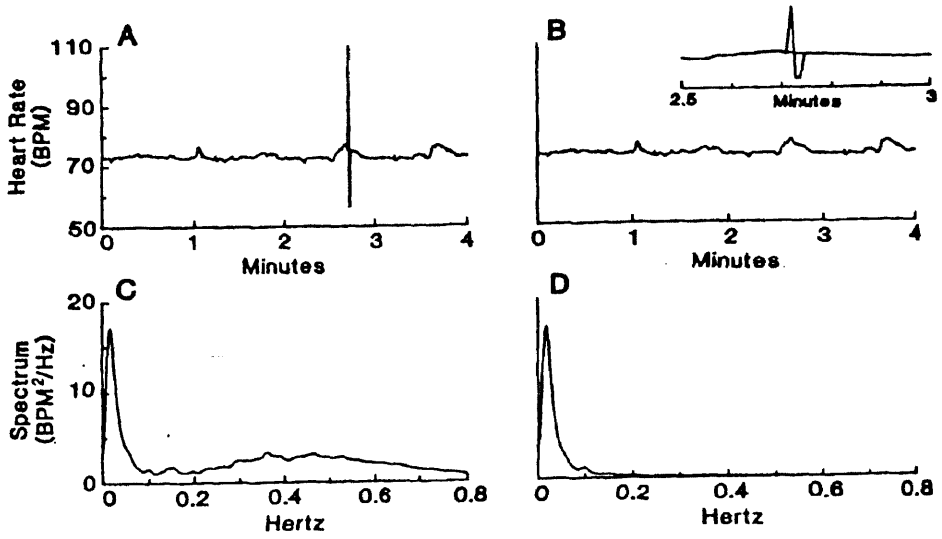

Figure 3.17 The affect of premature contraction on the HR spectrum. (a) A signal premature contraction causes an abrupt increase followed by a decrease in heart rate. (b) The premature contraction is removed from the heart rate data. (c) Poorly defined broad spectrum caused by impulse-like spike "artifact". (d) Spectrum of HR after impulse-like spike is removed.

In a similar way, the presence of a premature contraction could affect the spectrum of heart rate variability, and thus affect the estimation of vagal activity. In order to accurately estimate the vagal activity which is most important in this study, premature contractions in the EKG data have to be detected, removed and reconstructed. The detection of premature contraction beats is based on the assumption that the beat-to-beat variation in R-R intervals cannot exceed a critical percentage of the preceding interval, which is reasonable for the real data. The

basic algorithm is to compare each interbeat interval to the preceding one. If the difference in width exceeds a certain (80 percent is chosen in this study) percentage, a premature contraction beat is detected. In previous studies, the detected premature contractions were reconstructed manually, which caused many uncertainties. e.g. different people may reconstruct the beats at different places because of different individual experience or different judgment, same people also may reconstruct the beats differently at different time. In order to reduce the uncertainties and get a scientific and consistent method to reconstruct the premature beats, the cubic spline interpolation algorithm was examined.

Cubic spline interpolation is kind of nonlinear piecewise polynomial approximation. It divides a closed interval into a collection of subintervals and construct a different approximating polynomial on each subinterval[22]. cubic spline interpolation is the most common piecewise polynomial approximation using cubic polynomials between successive pairs of nodes. The definition of cubic spline interpolation is as follows: (see Figure 3.18)

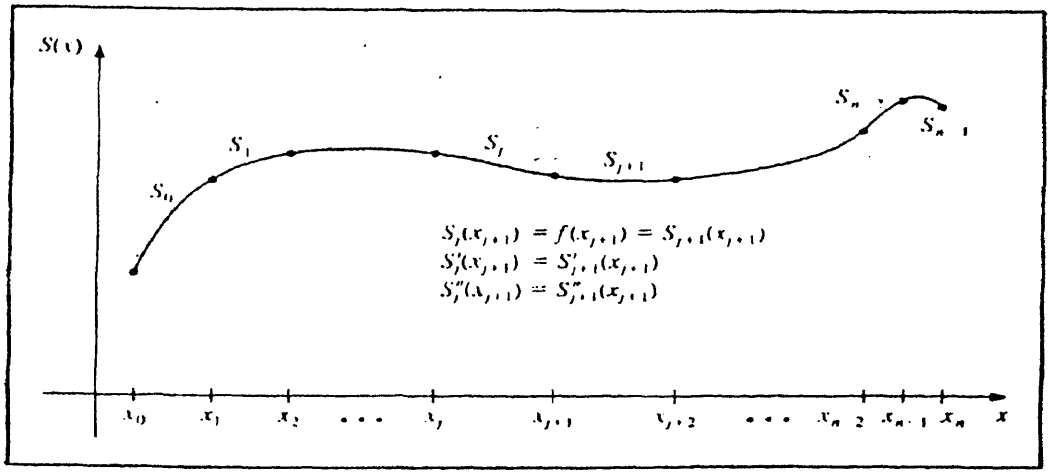

Figure 3.18 Cubic interpolation

Given a function f defined on [a,b] and a set of numbers, called nodes, $a = x_0 < x_1 ... < x_n = b$, a cubic spline interpolant, S, for f is a function that satisfies the following conditions:

a. S is a cubic polynomial, denoted s_j, on the subinterval $[x_j, x_{j+1}]$ for each j=0,1,...,n-1;

b. $s(x_j) = f(x_j)$ for each j=0,1,...,n-1;

c. $s_{j+1}(x_{j+1}) = s_j(x_{j+1})$ for each j=0,1,...,n-2;

d. $s_{j+1}'(x_{j+1}) = s_j'(x_{j+1})$ for each j=0,1,...,n-2;

e. $s_{j+1}''(x_{j+1}) = s_j''(x_{j+1})$ for each j=0,1,...,n-2;

f. one of the following set of boundary conditions is satisfied:

(i) $s''(x_0) = s''(x_n) = 0$ (free or nature boundary)

(ii) $s'(x_0) = f'(x_0)$ and $s'(x_n) = f'(x_n)$ (clamped boundary)

To construct the cubic spline interpolant for a given function f, the conditions in the definition are applied to the cubic polynomials.

$$s_j(x) = a_j + b_j(x - x_j) + c_j(x - x_j)^2 + d_j(x - x_j)^3 \quad \text{for each j=0,1,...,n-1} \qquad (4.1)$$

clearly,
$$s_j(x_j) = a_j = f(x_j) \qquad (4.2)$$

and if condition (c) is applied,

$$a_{j+1} = s_{j+1}(x_{j+1}) = s_j(x_{j+1}) = a_j + b_j(x_{j+1} - x_j) + c_j(x_{j+1} - x_j)^2 + d_j(x_{j+1} - x_j)^3 \qquad (4.3)$$

for each j=0,1...,n-2.

Since the term $(x_{j+1} - x_j)$ will be used repeated in this development, it is convenient to introduce the simpler notation

$$h_j = x_{j+1} - x_j \tag{4.4}$$

for each j=0,1,...,n-1. If we also define $a_n = f(x_n)$, then the equation

$$a_{j+1} = a_j + b_j h_j + c_j h_j^2 + d_j h_j^3 \tag{4.5}$$

holds for each j=0,1,...,n-1.

In a similar manner, define $b_n = s'(x_n)$ and observe that

$$s_j'(x) = b_j + 2c_j(x - x_j) + 3d_j(x - x_j)^2 \tag{4.6}$$

implies $s_j'(x_j) = b_j$ for each j=0,1,...,n-1. Applying condition (d)

$$b_{j+1} = b_j + 2c_j h_j + 3d_j h_j^2 \tag{4.7}$$

for each j=0,1,...,n-1.

Another relation between the coefficients of s_j is obtained by defining $c_n = s''(x_n)/2$ and applying condition (e). In this case

$$c_{j+1} = c_j + 3d_j h_j \tag{4.8}$$

for each j=0,1,...,n-1.

Solving for d_j in Eq.(4.8) and substituting this value into (4.5) and (4.7) gives the new equations.

$$a_{j+1} = a_j + b_j h_j + \frac{h_j^2}{3}(2c_j + c_{j+1}) \tag{4.9}$$

and

$$b_{j+1} = b_j + h_j(c_j + c_{j+1}) \tag{4.10}$$

for each j=0,1,...,n-1.

The final relationship involving the coefficients is obtained by solving the appropriate equation in the form of equation (4.9), first for b_j.

$$b_j = \frac{1}{h_j}(a_{j+1} - a_j) - \frac{h_j}{3}(2c_j + c_{j+1}) \tag{4.11}$$

and then, with a reduction of the index, for b_{j-1},

$$b_{j-1} = \frac{1}{h_{j-1}}(a_j - a_{j-1}) - \frac{h_{j-1}}{3}(2c_{j-1} + c_j) \tag{4.12}$$

Substituting these values into the equation derived from Eq.(4.10), when the index is reduced by 1, gives the linear system of equations.

$$h_{j-1}c_{j-1} + 2(h_{j-1} + h_j)c_j + h_j c_{j+1} = \frac{3}{h_j}(a_{j+1} - a_j) - \frac{3}{h_{j-1}}(a_j - a_{j-1}) \tag{4.13}$$

for each j=1,2,...,n-1. This system involves, as unknowns, only $\{c_j\}_{j=0}^{n}$, since the value of $\{h_j\}_{j=0}^{n-1}$ and $\{a_j\}_{j=0}^{n}$ are given by the spacing of nodes $\{x_j\}_{j=0}^{n}$ and the values of f at the nodes.

Note that once the values of $\{c_j\}_{j=0}^{n}$ are known, it is a simple matter to find the remainder of the constants $\{b_j\}_{j=0}^{n-1}$ and $\{d_j\}_{j=0}^{n-1}$ and to construct the cubic polynomials $\{s_j\}_{j=0}^{n-1}$.

First, the advantages of cubic spline interpolation are: it is a piecewise polynomial interpolation. For the non-piecewise polynomial interpolation algorithms, the approximation of arbitrary functions is made on closed intervals by the use of polynomials. The oscillatory nature of high-degree polynomials and the property that a fluctuation over a small portion of the interval can induce large fluctuations over the entire range restrict their use in many situations.

Second, cubic spline interpolation is a non-linear piecewise polynomial approximation. Although linear piecewise polynomial approximation is easier to apply than the non-linear piecewise approximation, the big disadvantage of linear approximation is that at each of the endpoints of the subintervals these is no assurance of differentiability, which, in a geometrical context, means that the

interpolating function is not "smooth" at these points. Often it is clear from physical conditions that such a smoothness condition is required and that the approximation function must be continuously differentiable. Since interbeat interval is a non-linear system, a non-linear interpolation could fit data more accurately than a linear interpolation. A general cubic polynomial involves four constants (a_j, b_j, c_j, d_j), so there is sufficient flexibility in the cubic spline procedure to ensure not only that the interpolant is continuously differentiable on the interval, but also that has a continuous second derivative on the interval. Also, the linear interpolation may reduce the fluctuation in the data. If the linear interpolation is used to interpolate the interbeat interval, it may result in less heart rate variability, and thus may cause the detected vagal activity to be less than it should be.

In S-Plus, the procedure of reconstructing premature contractions using cubic spline interpolation is very simple. When a premature contraction occurs, the interval between the premature beat and the preceding beat is shorted, and the interval between the premature beat and the next succeeding beat is prolonged. The shortened and the prolonged intervals are represented as an exceptionally small followed by an exceptionally large interval value. These two values need to be removed before cubic polynomial interpolation is performed. The removing procedure could be done manually. After all the irregular intervals caused by premature contractions are removed, cubic polynomial interpolation is performed on the series which contains the remaining normal interbeat intervals by using the "spline" algorithm existing in S-Plus. Afterwards, the corresponding interpolated

values are used to replace the abnormal intervals caused by premature beats in the original interbeat interval series. Since premature contractions may occur continuously, this may result in more than two abnormal interval values appearing continuously. All these abnormal interval data have to be removed before performing the cubic spline interpolation. In this case, the number of points needed to be interpolated between each pair of interval values is determined by the number of points that have been continuously removed. Figure 3.19 demonstrates a group of interbeat intervals of an EKG signal collected from a normal subject. The x-axis represents index number and the y-axis represents the interbeat interval values. Figure 3.19 (a) demonstrates the original interbeat intervals which contain premature contractions, while Figure 3.19 (b) demonstrates the reconstructed interbeat intervals using the cubic spline interpolation algorithm, and Figure 3.19 (c) demonstrates the reconstructed R peak position represented by the vertical lines in the original EKG data..

Although the cubic polynomial is a simple, powerful algorithm suggested in this study to handle R-R interval data that contain occasional premature contractions, it must be stressed that the characteristics of the data are changed no matter what kind of algorithms are used; thus, it is preferable to use data segments that are free from premature contractions.

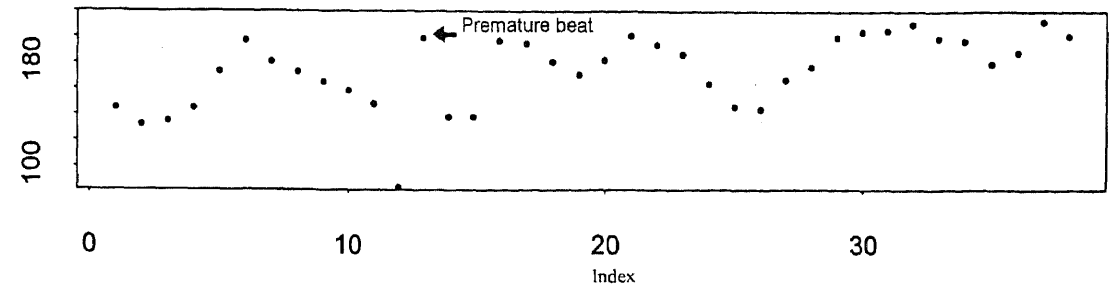

(a)

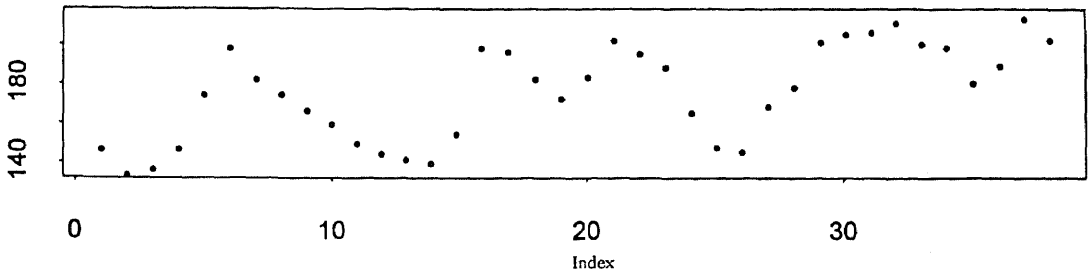

(b)

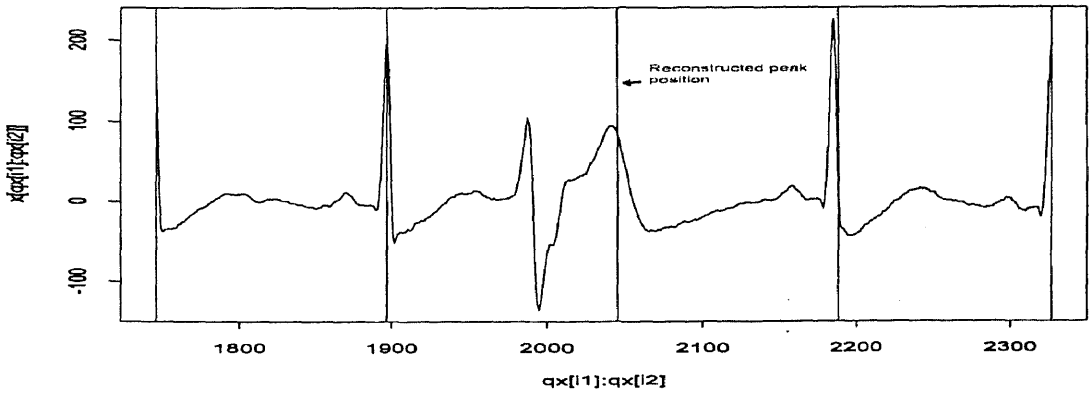

(c)

Figure 3.19 Premature beat reconstruction. (a) A interbeat intervals series which contains a premature beat. (b) The same interbeat intervals in which premature beat has been reconstructed. (c). The reconstructed peak position in the original EKG data.

CHAPTER 4

DISCUSSION AND CONCLUSIONS

4.1 Low Vagal Activity in Stroke Survivors

As discussed in section 1.2, it is clear that, in the power spectral analysis of heart rate variability, the respiration peak corresponding to the RSA is purely parasympathetic in origin. Individual differences of area values under respiration peaks have been interpreted as differences in basal cardiac vagal tone, and within subjects changes of area values under respiration peaks have been suggested to correspond to alterations in vagal tone. Stroke survivor test results shown in Table 3.1 demonstrated that the HRV power values within the respiration peak is much lower in stroke survivors than that in normal controls. This suggests that the stroke survivors have significantly less parasympathetic reserve than the control subjects. The result is consistent with the previous pilot work performed by Seshadri and Reisman[23]. As a continuation of their study, the contribution of this study is that Holter recorder is used to collect all the EKG data from the subjects and the subject's age and gender are matched during the test. Both the using of a Holter recorder and the age matching bring a more powerful evidence to illustrate that stroke survivors have less vagal activity than the normal controls. Since it has been shown that aging results in an attenuation of vagal-cardiac activity[24], therefore, without age matching, the evidence becomes less powerful. Also, using a Holter

recorder to collect data could reduce the laboratory effect, and therefore, reduce subject's mental stress, which also affects vagal activity.

The reasons that stroke survivors have less parasympathetic activity than normal people are not quite clear. Our hypothesis is that cardiac autonomic innervation originates in the brain stem (parasympathetic) and spinal (sympathetic) nuclei. Damage may be caused in one or more of these areas in stroke survivors. If one or more of the areas believed to be involved with autonomic function are damaged, this may cause a change in autonomic activity and result in a decrease of parasympathetic activity. Studies showed that vagal activity in humans was significantly decreased in patients with brain stem as well as hemispheric lesions[25] acutely after stroke. The reason for low vagal activity in stroke survivors has to be further investigated.

In all subjects, HRV power was significantly lower and virtually non-existent in some cases during EXERCISE. HRV power during NON-PACED breathing was lower than that of PACED breathing at 8bpm. This suggested that exercise might not be required to assess cardiac function in stroke survivors, but paced breathing should be strongly considered when HRV is assessed. This observation needs to be further investigated.

4.2 Less Heart Rate Variations in Stroke Survivors

The box plot discussed in section 3.1.2 is a simple graphic representation showing the center and spread of a distribution, along with a display of unusually deviant data points, called outliers. Box plots provide a very powerful method for

visualizing the rough distribution shape of two samples of data. The box plots of the IBIs from both controls and stroke survivors showed significantly larger distribution of IBIs in the controls than that in the stroke survivors, which suggested that heart rate fluctuates more in controls than that in stroke survivors. This result was in agreement with the result shown in section 4.1 that stroke survivors had lower vagal activity than controls.

It is clear that, although inherent rhythmicity of the heart is due to a natural pacemaker situated in the sinoatrial node, continuous beat-to-beat control of heart rate is dependent on the relative balance between sympathetic and parasympathetic nerve impulses delivered from the brain to the SA node. The parasympathetic nervous system directly mediates short-term heart rate variations, thus, decreased vagal tone may contribute to the reduced beat-to-beat variation. Furthermore, increased sympathetic activation can reduce short-term heart rate variability by inhibiting vagal activation of the heart. Thus, either sympathetic hyperactivity or parasympathetic hypoactivity, or some interaction of the two, may underlie the reduced beat-to-beat heart variation. In stroke survivors, there was a sustained low variation of heart rate suggesting that stroke survivors may suffer from one or more aspects of autonomic nervous system imbalance.

4.3 Vagal Activities Change with the Respiration Rate

We have observed that vagal activities related to respiration rate changed for both control subjects and stroke survivors. With the exception of 58/M in the stroke survivor group, HRV power during NON-PACED: sitting and supine was lower

than that of PACED: 8bpm in all subjects. This reflected an increase of HRV power resulting from ventilating approximately at the frequency of ventilatory sinus arrhythmia. In addition, with exception of 60/M in the normal group, HRV power decreased progressively in all subjects during PACED: 8bpm, 12bpm and 18bpm. In 1990, Walker showed that hypoxia increased heart rate due to a predominance of the cardiac sympathetic over cardiac vagal activation.[12] Hyperoxia resulted in bradycardia from decreased cardiac sympathetic nerve discharges. Hypocapnia caused a cardioaccelatory response due to local effect on heart rate despite significant increased in cardiac vagal discharges. Hypercapnia excited cardiac sympathetic and inhibited cardiac vagal activity. The progressively decreased HRV power in all subjects during PACED: 8bpm, 12bpm, and 18bpm reflected the effect of hypocapnia.

4.4 Vagal Withdrawal with Audience

It is known complex social factors can influence physiological activity, behavior, and health, but little is known about how essential components of these factors (e.g. human association, observation) affect human physiology. The major finding of the oral presentation test was that high frequency range area values diminished significantly during the presentation in presence of an audience, when compared to high frequency areas during a presentation without an audience. It is also found that, in some cases, the high frequency range area values during the anticipation of making a presentation were lower than those during the presentation without audience. The result showed the interference of the presence of an audience on the

autonomic behavior. Due to the uncertainty created by an audience, the presence of an audience increased the subject's "arousal" level which results in the decrease of the subject's parasympathetic activity. The effects of an audience on the power spectrum of HRV may be interpreted as follows: first, subjects had a fright stage of appearing in front of an audience. Second, subjects were anxious about presenting their data in the presence of a critical and evaluative audience. Changes of parasympathetic activity revealed greater activation during a task under audience over under no-audience conditions. The social psychological influence resulted in signficantly vagal tone withdrawal in the presence of an audience.

Within our sample we noticed high and low autonomic reactors. Due to the small number of participants, we did not attempt to separate these two groups. In this study, we failed to detect a reciprocal sympathetic activation during a parasympathetic withdrawal. This is partly due to the unknown contributions of autonomic and physiological processes modulating the low frequency component.

CHAPTER 5

FUTURE WORK

Power spectral analysis of heart rate variability is a potentially powerful tool for exploring neurocardiac dysfunction in patients with a variety of cardiac and autonomic disorders. In this study, pilot data have been obtained from stroke survivor tests as well as oral presentation tests in which power spectral analysis of HRV has been applied. In the following, some suggestions have been proposed for future work:

1)The EKG-derived respiration method needs to be tested further. In the stroke survivor test, although respiration signals were derived from the Holter EKG signal of all subjects from all tests, the respiration signals were only treated as a reference, and were not used to determined the high frequency (respiration) peaks in the spectrum of HRV. This is because the correlation between Holter EKG derived respiration and original respiration has not been tested accurately. It has been proved that the regular EKG derived respiration is strongly associated with the original respiration, However, due to the distortion of Holter EKGs caused by the play back system, the spectrum of the respiration derived from the Holter EKGs has been distorted by some degree. Although in Zhao and Reisman's study, it was shown that the overall correlation coefficient of the central frequencies of the derived and original respiration spectra for Holter data from 3 normal subjects was 0.9965[13], it was not sufficient to prove that the respiration derived from the Holter EKGs is strongly correlated with the original respiration, because their

Holter EKGs is strongly correlated with the original respiration, because their sample is very small (only 3 subjects). The correlation of the respiration derived from the Holter EKGs with the original respiration could be tested by comparing spectra of both signals. The experimental protocol for this purpose could follow the routine experimental protocol designed in the investigation of heart rate variability for stroke survivors performed at the Kessler Institute for Rehabilitation, which includes the collection of two lead EKG signals (leads I and III)and respiration on healthy subjects during different test conditions. such as 1) rest, non-paced breathing, 2) rest, paced breathing at different rates, 3) exercising at different levels, and 4) recovery. The respiration data needs to be collected simultaneously with the EKG data. The respiration wave could be recorded using impedance pneumography. The basic working principle of the impedance pneumography is to apply a constant high frequency current to the chest and the resulting voltage reflecting the impedance changes due to the filling and emptying of the lungs during respiration is detected.

After EKGs and respiration data are collected under different test conditions, respiration signals could be derived from the two lead EKGs using the EKG derived respiration algorithm, and the spectra of derived respiration as well as the spectra of original respiration could be derived. Then, the distortion of the derived respiration could be tested by performing the cross correlation between the derived respiration and the original respiration.

2) The stroke survivor study should be continued. The stroke survivor project is a long term study. The major purposes of this study are a) to determine whether

HRV is related to current functional limitations and is a significant factor in predicting functional outcome. b) to determine the efficacy of HRV in the prediction of cardiac complications after stroke. The current pilot data only demonstrated different vagal activities between normal controls and stroke survivors. In order to reach the major purpose, the protocol will need to be improved, for example, the information during recovery period after exercise should be recorded so that the activity of the autonomic nervous system after exercise could be understood. More stroke survivors will need to be recruited to be evaluated at particular time intervals after stroke onset.

3) The oral presentation test is also an unfinished study. The pilot data of the oral presentation test only revealed the fact that vagal activity diminished significantly with the anticipation of making a presentation as well as during the presentation in the presence of an audience, when compared to vagal activity during a presentation without an audience. With increasing sample size, we might be able to decide whether subjects have high or low "autonomic" reactors, or we might be able to decide whether the evoked response during an oral presentation test reduces overall cardiovascular health.

APPENDIX A

PROCEDURE FOR CALCULATING VAGAL ACTIVITY

In the following, we are going to use a sample data file t199.asc to explain the syntax of the programs used to calculate vagal activity. t199.asc file contains two columns EKG data: 1) lead I and 2) lead III. The length of each column in the file t199 in S-Plus is assumed to be 30003

1 Converts data file from ASCII code into S code.
t199_matrix(scan("_data\\t199.asc",sep=",",skip=1),ncol=2,byrow=T)

2 Cuts the beginning and the end of the file.
t199.c_t199[3:30000,]

3 Detects R peaks in the EKG data.
t199.l_htlws(t199.c[,2])

4 If miss detection is present, use **mqrs** to detect the missed R peaks manually until all R peaks are detected.
t199.m_mqrs(t199.c[,2],t199.l$pk,pout(diff(t199.l$pk)))

5 If double detection is present, use **dqrs** to delete all double detected R peaks.
a) If changes were made in **mqrs**.
t199.d_dqrs(t199.c[,2],t199.m)

b) If changes were not made in **mqrs**.
t199.d_dqrs(t199.c[,2],t199.l$pk)

7 Makes final file
a) If no changes were made in **dqrs** or **mqrs.**
t199.fin_t199.l

b) If changes were made in **dqrs** or **dqrs+mqrs.**
t199.fin_fworkbh(t199.d)

c) If no changes were made in **dqrs**, but changes were made in **mqrs.**
t199.fin_fworkbh(t199.m)

8 Calculates vagal activity.
t199.area_spect1(t199.fin$isp,low.freq=##, High.freq=##, srate=200)

APPENDIX B

PROCEDURE FOR DERIVING RESPIRATION FROM EKG

In the following, the commands of programs used to derived respiration from EKG is going to be explained. Before deriving respiration from EKG, the procedures in Appendix A must be completed.

1 Calculates the areas under QRS complexes in the EKG from lead I.
t199.qr1_qrsca(t199.c[,1],t199.fin$pk)

2 Calculates the area under QRS complexes in the EKG from lead III.
t199.qr3_qrsca(t199.c[,2],t199.fin$pk)

3 Calculates the angle of the cardiac electrical vector axis
t199.du_duall(t199.qr1,t199.qr3)

4 Generates derived respiration signal
t199.dr_edr(t199.du)

5 Generates the spectrum of derived respiration signal.
t199.fn_fsph(t199.dr)

APPENDIX C

S-PLUS PROGRAMS

1. FRPK

```
function(x, zf = 15, mindiff = 50, qhg = 0.25, zdelta =
 0, tooruff
         = 0.8, hash = 30)
{
#x: ecg signal
        x.pk <- lwzx(x, f = zf, mindiff = mindiff, qx =
 qhg, delta
                 = zdelta, hash = hash)
        pk <- x.pk$pk
        ibi <- diff(pk)
        mruff <- max(abs(ruff(ibi)))
        if(mruff >= tooruff) {
                print(paste("IBI'S MAY BE TOO RUFF"))
                print(paste("MAX IBI IS", max(ibi), "["
, (1:length(
                        ibi))[ibi >= max(ibi)], "]"))
                print(ibi)
        }
        pk
}
```

```
                                        )] + bb
                                    abline(v = tx, lty = 2)
                                    cx <- c(cx, tx)
                            }
                    }
            }
            print(cx)
            for(i in 1:length(cx)) {
                    qxu <- qx[qx < cx[i]]
                    qxo <- qx[qx > cx[i]]
                    qx <- c(qxu, cx[i], qxo)
                    print(length(qx))
            }
#qfx <- list(qx = qx, ibi=diff(qx))
            qfx <- qx
            qfx
}
```

3.QRSCA

```
function(x, pkx, ac = 7, k = 2)
{
#x:ecg data(col 2), pkx: R peak, hwin:
        hwin_ac
        if(pkx[1] < hwin) {
                pkx <- pkx[2:length(pkx)]
        }
        if(length(x) < (pkx[length(pkx)] + 3 * hwin)) {
                pkx <- pkx[1:(length(pkx) - 1)]
        }
        lwf <- lowess(1:length(x), x, f = 45/length(x),
 iter = 2,
                delta = 0.1)$y
        x <- x - lwf
        minx <- vector("numeric", 0)
        for(i in 1:length(pkx)) {
                minx1 <- ((pkx[i] - hwin):pkx[i])[(x[(p
kx[i] -
                        hwin):pkx[i]]) <= min(x[(pkx[i]
 - hwin):
                        pkx[i]])]
                if(length(minx1) > 1) {
                        minx1 <- minx1[length(minx1)]
                }
                minx <- c(minx, minx1)
        }
        if(length(pkx) != length(minx)) {
                print(paste("Number of Q's is not equal
 to that of R's"
                        ))
                print(paste("Q's:", length(minx)))
                print(paste("R's:", length(pkx)))
                stop()
        }
        shwd <- round(mean(pkx - minx) * k)
        qrsca <- vector("numeric", 0)
        for(i in 1:length(minx)) {
                cols <- x[(minx[i] + 1):(minx[i] + shwd
)]
                ca1 <- sum(cols)
```

```
                dft <- x[minx[i]] * shwd
                rca <- cal - dft
                qrsca <- c(qrsca, rca)
        }
        par(mfrow = c(1, 1))
        plot(qrsca)
        z <- list(qrsca = qrsca, pkx = pkx, x = x, minx
 = minx)
        z
}
```

4. RMBQ

```
function(x)
{
#x:output of qrsca
        x1 <- x$qrsca
        x2 <- x$pkx
        plot(x1)
        xs <- 1:length(x1)
        bqa <- identify(xs, x1, plot = T)
        j <- 0
        for(i in 1:length(bqa)) {
                x2 <- x2[ - (bqa[i] - j)]
                j <- j + 1
        }
        x2
}
```

5. DUALL

```
function(x1, x2)
{
#x1:first lead qrsca;x2:second lead qrsca
        qca1 <- x1$qrsca
        qca2 <- x2$qrsca
        qrsca <- atan(qca1/qca2)
        z <- list(qrsca = qrsca, pkx = x1$pkx)
        z
}
```

6. EDR

```
function(x)
{
# x: output of qrsca
        pkx <- x$pkx
        qrsca <- x$qrsca
        n <- pkx[length(pkx)] - pkx[1] + 1
        iedr <- spline(pkx, qrsca, n)
        sted <- c(iedr$x[1], iedr$x[length(iedr$x)])
        z <- list(iedr = iedr$y, sted = sted)
        z
}
```

7. FSP

```
function(x1, x2, title = "", f2 = 0.2)
{
#x1: resp signal; x2: edr output
        orresp <- x1
        edresp <- x2$iedr
        stp <- x2$sted[1]
        edp <- x2$sted[2]
        orresp <- orresp[stp:edp]
        d.orp <- orresp[seq(1, length(orresp), 10)]
        d.orpl <- lowess(1:length(d.orp), d.orp, f = 0.
3, iter = 2,
                delta = ceiling((length(d.orp) * 0.3)/8
))$y
        d.orps <- spect(d.orp - d.orpl, nt = 8192, ns =
 6)
        d.edr <- edresp[seq(1, length(edresp), 10)]
        d.edrl <- lowess(1:length(d.edr), d.edr, f = f2
, iter = 2,
                delta = ceiling((length(d.edr) * 0.3)/8
))$y
        d.edrs <- spect(d.edr - d.edrl, nt = 8192, ns =
 6)
        z <- list(d.orp = d.orp, d.edr = d.edr, d.orps
= d.orps[1:
                330], d.edrs = d.edrs[1:330])
        z
}
```

8. DGF

```
function(x, title = "")
{
#x: output if fsp
        d.orp <- x$d.orp
        d.edr <- x$d.edr
        d.orps <- x$d.orps
        d.edrs <- x$d.edrs
        xf <- ((1:330) - 1)/8192 * 20
        dev.set(which = 2)
        par(mfrow = c(2, 1), mar = c(4, 5, 3, 1))
        plot(d.orp, type = "l", main = paste(title, "-O
riginal"))
        plot(d.edr, type = "l", main = paste(title, "-D
erivation")
                )
        dev.set(which = 3)
        par(mfrow = c(2, 1), mar = c(4, 5, 3, 1))
        plot(xf, d.orps[1:330], type = "l", xlab = "Fre
quency(Hz)",
                ylab = "Power", main = paste(title, "-O
riginal"))
        plot(xf, d.edrs[1:330], type = "l", xlab = "Fre
quency(Hz)",
                ylab = "Power", main = paste(title, "-D
erivation")
                )
}
```

9.SPCP

```
function(x, h = 0.3, nt = 8192, sr = 20, f1 = 1, f2 = 1
00)
{
#x:output of fsp
        fn <- sr/(nt * 3)
        x1 <- x$d.orps
        x2 <- x$d.edrs
        xscal <- 1:330
        x1 <- spline(xscal, x1)$y
        x2 <- spline(xscal, x2)$y
        f1 <- round(length(x1) * (f1/100))
        f2 <- round(length(x1) * (f2/100))
        x1.c <- x1[f1:f2]
        x2.c <- x2[f1:f2]
        x1.mc <- (1:length(x1.c))[(x1.c >= max(x1.c))]
        x2.mc <- (1:length(x2.c))[(x2.c >= max(x2.c))]
        x1.m <- x1.mc + f1 - 1
        x2.m <- x2.mc + f1 - 1
        x11.r <- rev(x1[1:x1.m])
        x12 <- x1[x1.m:length(x1)]
        x21.r <- rev(x2[1:x2.m])
        x22 <- x2[x2.m:length(x2)]
        f1.lr <- fm1(x11.r, x1[x1.m] * h)
        f1.l <- x1.m - f1.lr + 1
        f1.hm <- fm1(x12, x1[x1.m] * h)
        f1.h <- x1.m + f1.hm - 1
        f2.lr <- fm1(x21.r, x2[x2.m] * h)
        f2.l <- x2.m - f2.lr + 1
        f2.hm <- fm1(x22, x2[x2.m] * h)
        f2.h <- x2.m + f2.hm - 1
        a1 <- sum(x1[f1.l:(f1.h - 1)])
        a2 <- sum(x2[f2.l:(f2.h - 1)])
        ai.1 <- a1/(x1[x1.m] * (f1.h - f1.l))
        ai.2 <- a2/(x2[x2.m] * (f2.h - f2.l))
        ha1.sm <- x1[f1.l]
        for(i in (f1.l + 1):f1.h) {
                ha1 <- x1[i]
                ha1.sm <- sum(ha1.sm, ha1)
                if(ha1.sm >= (a1/2)) {
                        cf1 <- (1:length(x1))[(x1 == x1
```

```
[i])]
                        break
                }
        }
        ha2.sm <- x2[f2.l]
        for(i in (f2.l + 1):f2.h) {
                ha2.sm <- sum(ha2.sm, x2[i])
                if(ha2.sm >= a2/2) {
                        cf2 <- (1:length(x2))[(x2 == x2
[i])]
                        break
                }
        }
        z <- list(f1 = c(f1.l, f1.h, cf1) * fn, f2 = c(
f2.l, f2.h,
                cf2) * fn, ra = c(ai.l, ai.2))
        z
}
```

REFERENCES

1. C. Guyton. *Textbook of Medical Physiology*. Philadelphia: W.B. Saunders Company. Eighth Edition. 1990.

2. J. Wartak. *Simplified Vectorcardiography*. Philadelphia: J. B. Lippincott Company. 1970

3. A. J. Vander, J. H. Sherman, D. S. Luciano. *Human Physiology*. McGraw-Hill Publishing Company. Fifth Edition. 1990

4. A. L. Goldberger, D. R. Rigney, and B. J. West. "Chaos and Fractals in Human Physiology" *Scientific American*. 262: 42-49,1990

5. M. Pagani, G. Malfatto, S. Pierini, R. Casati, A. M. Masu, M. Poli, F. Guzzetti, F. Lombardi, S. Cerutti, and A. Malliam. "Spectral Analysis Heart Rate Variability in the Assessment of Autonomic Diabetic Neuropathy" *Journal of Autonomic Nervous System*. 23: 143-149, 1988.

6. R. E. Kleiger, J. P. Miller, J. T. Jr. Bigger, A. J. Moss and the Multicenter Post-Infarction Research Group. "Decreased Heart Rate Variability and Its Association With Increased Mortality After Acute Myocardial Infarction" *American Journal of Cardiology*. 59: 256-264, 1987.

7. J. T. Jr. Bigger, R. E. Kleiger, J. L. Fleiss, L. M. Rolintzky, R. C. Steinman, J. P. Miller, and Multicenter Post-Infarction Group. "Components of Heart Rate Variability Measured During Healing of Acute Myocardial Infarction" *American Journal of Cardiology*. 61: 208-215, 1988.

8. M. V. Kamath, E. L. Faller. "Power Spectral Analysis of Heart Rate Variability: A Noninvasive Signature of Cardiac Autonomic Function" *Critical Reviews in Biomedical Engineering*. 245-310, 1993.

9. S. Akselrod, D. Gordon, F. A. Ubel, D. C. Shannon, A. C. Barger, and R. J. Cohen. "Power Spectrum Analysis of Heart Rate Fluctuation: A Quantitative Probe of Beat-to-Beat Cardiovascular Control" *Science*. 213: 220-223,1989

10. R. I Kithey. "An Analysis of the Nonlinear Behavior of the Human Thermal Vasomotor Control System" *Journal of Theoretical Biology*. 52: 231-248,1975.

11. G. G. Berntwon, J. T. Cacioppo, and K. S. Quigley. "Respiratory Sinus Arrhythmia: Autonomic Origins, Physiological Mechanisms, and Psychophysiological Implications" *Psychophysiology*. 30: 183-196, 1993.

12. S. J. Shin, W. N. Tapp, S. S. Reisman, and B. H. Natelson. "Assessment of Autonomic Regulation of Heart Rate Variability by the Method of Complex Demodulation" *IEEE Transaction on Biomedical Engineering*. 36(2): 274-282,1989.

13. L. Zhao, S. Reisman, T. Findleyl "Respiration Derived from the Electrocardiogram During Heart Rate Variability Studies" *IEEE Engineering in Medicine and Biology Society*. 123-124. 1994

14. J. T. Jr. Bigger, J. L. Fleiss, R. C. Steinman, L. M. Rolnitzky, R. E. Kleiger and J. N. Rottman. "Frequency Domain Measures of Heart Period Variability and Mortality After Myocardial Infarction" *Circulation*. 85: 164-170,1992.

15. L. Fei, M. H. Anderson, D. Katritsis, J. Sneddon, D. J. Statters, M. Malik, A. J. Camm. "Decreased Heart Rate Variability in Survivors of Sudden Cardiac Death not Associated with Coronary Artery Disease" *British Heart Journal*. 71(1): 16-21, 1994

16. D. G. Sherman, R. G. Hart, F. Shi. "Heart-Brain Interactions: Neurocardiology or Cardioneurology Comes of Age" *Mayo Clinic Proceeding*. 62: 1158-1160, 1987.

17. E. J. Roth, K. Mueller, D. Gren. "Stroke Rehabilitation: Cardiovascular Response to Phusical Thrapy" *Neurorehabilitation*. 2(2): 7-15, 1992.

18. J. T. Cacioppo, P. A. Rourke, B. S. Marshall-Goodell, L. G. Tassinary, and R. S. Baron. "Rudimental Physical Effects of Mere Observation" *Psychophysiology*. 27: 177-186, 1990.

19. J. P. Saul. "Beat-to-Beat Variations of Heart Rate Reflect Modulation of Cardiac Autonomic Outflow" *NIPS* 5: 32-36, 1990.

20. L. Zhao. "Derivation of Respiration from Electrocardiogram During Heart Rate Variability Studies" *MS. Thesis, New Jersey Institute of Technology*, May, 1994.

21. J. P. Saul, Y. Arai, R. D. Berger, L. S. Lilly, W. S. Colucci, R. J. Cohen. "Assessment of Autonomic Regulation in Chronic Congestive Heart Rate Failure by Heart Rate Spectral Analysis" *American Journal of Cardiology.* 61: 1292-1298, 1988.

22. R. L. Burden, J. D. Faires. *Numerical Analysis.* Boston: PWS-KENT Publishing Company. Fourth Edition. 1989.

23. K. Seshadri, S. Reisman, M. Daum, R. Zorowitz, R. DeMeersman. "Heart Rate Variability in Stroke Population and Normal: A Comparison Using Spectral Analysis" *Proceeding of the 1994 20th Annual Northeast Bioengineering Conference.* 10-13, 1994

24. R. E. DeMeersman. "Aging as a Modulator of Respiratory Sinus Arrhythmia" *Journal of Gerontology: Biological Sciences.* 48(2): B74-B78, 1993.

25. S. A. Barron, Z. Rogovaki, J. Hemli. "Autonomic Consequences of Cerebral Hemisphere Infarction" *Stroke.* 25: 113-116, 1994.

26. P. V. O'Neil. *Advanced Engineering Mathematics.* California: Wadsworth Publishing Company. Third Edition. 1991.

27. R. C. Gonzalez, R. E. Woods. *Digital Image Processing.* Addison-Wesley Publishing Company. 1992.